NTNU
Norwegian University of
Science and Technology

SIEMENS
Ingenuity for life

SPECIALIZATION PROJECT

Identification of Key Parameters and Potential Solutions for Smarter Charging of Battery Ferries

Morten Volland Finnekås

Abstract

To reach the national plan for reduction in greenhouse gas emissions, a revolution in the Norwegian ferry operation has taken place over the last years. By using batteries instead of diesel generators for ferry operation, an equivalent annual emission from 150,000 cars can be reduced in near future.

One key problem to investigate is how to smarter plan the charging of such battery ferries. Today's charging pattern is mainly focusing on transferring the most energy in the shortest possible time, but a future charging plan could take into account many factors for more effective charging.

This report is identifying some of the important factors regarding operation and charging of ferries and proposes a methodology for controlling the charging based on electricity pricing and weather conditions.

While there is a lack of literature aiming directly at the problem, research in the field of electric vehicles and charging of lithium-ion batteries are used to support the material in the report.

A brief overview of the history, different configurations and characteristics of a battery ferry is given, and important factors regarding the origin of battery ageing phenomena and proposals for achieving greater battery lifetime are discussed.

A system consisting of a battery ferry crossing between two charging stations connected to local grids are modelled in Simulink. The first study case is using a controller taking the weather conditions into account and the second study case is using a controller considering the electricity pricing.

In the first study case, the batteries in the two charging stations are more utilized due to more energy consumption in the ferry. In the second study case, results shows that cost savings can be made by adjusting the amount of energy transferred throughout the day.

Future work should emphasize on better modelling of the system, with more advanced weather and load models, and the development of a more dynamic charge controller.

Preface

This report presents the work done in the course TTK4550 - Specialization Project at the Department of Engineering Cybernetics, Norwegian University of Science and Technology (NTNU). The work has been done in the period from August to December 2018.

The problem description for this specialization project is formulated by Siemens Offshore Marine Center in Trondheim, which has also contributed with relevant data and discussions.

The purpose of the project has been on identifying important factors and strategies related to smarter charging of battery ferries and reflect upon future opportunities and challenges. As a master thesis will be a continuation of this specialization project, obtaining relevant background knowledge in the field of ferry operation has also been a focus.

Acknowledgement must be given to the supervisors for their good answers, relevant discussions and thoughts on the problem which has greatly improved the student's knowledge and ability to achieve the results in the report.

Lastly, the student would like to thank Siemens in Trondheim for giving the opportunity to work on relevant and interesting problems in an industry which is actively seeking solutions for a more sustainable environment.

Acronyms

In alphabetical order:

AC   Alternating Current
BESS   Battery Energy Storage System
CMS   Charge Management System
DC   Direct Current
DoD   Depth of Discharge
DPS   Dynamic Position System
ESM   Energy Storage Module
ESS   Energy Storage System
IAS   Integrated Automation System
IPS   Integrated Power System
ODE   Ordinary Differential Equation
PDE   Partial Differential Equation
PEBB   Power Electronic Building Block
PEM   Power Electronics Module
PMS   Power Management System
RCS   Remote Control System
RTE   Round Trip Efficiency
SEI   Solid Electrolyte Interphase
SoC   State of Charge
SoH   State of Health
VSC   Voltage Source Converter
VSD   Variable Speed Drive

Contents

List of Tables

List of Figures

Chapter 1

Introduction

This introductory chapter will provide background context on and motivation for smarter charging of battery ferries. Both technical and social aspects on the current situation for battery ferry's will be enlightened and used as a basis for the problems to be solved.

Since the system to be considered involves high complexity and a large variety of impacting factors, assumptions and limitations used to simplify the system are discussed. Delimitations are also given to limit the scope of the problem and to define the boundaries of the study.

Further, a literature review will present the relevant knowledge and work on this topic. The literature review will be divided into two parts, where the first part is considering the literature on hybrid ferry systems and the second part is considering the literature on battery life management.

Finally, the achievements for the work done in this study and the background contributions are presented.

1.1   Motivation

"The Norwegian Parliament asks the Government to make sure that all future ferry tenders meets a demand for zero-emission technology (and low - emission technology) when this is indicated by the technology"

Approved proposal, Budget agreement fall 2014 [17]

People and villages are connected to the outside society and national roads are connected together through the use of ferries. Today there are about 180 ferries that includes as an important and necessary part of the Norwegian transportation infrastructure, and almost all of them are powered by diesel generators. This causes the ferries to be one of the highest contributors to climate pollution in the transportation sector[18].

To reach the climate goal sat by the Norwegian Parliament, that greenhouse gas emissions shall be reduced by at least 40 % from the reference year 1990 by 2030 [19], something must be done in the transportation sector. For the ferries, this challenge has marked the beginning of a new era. Since the first battery operated car ferry, Ampere, was commissioned and put into operation in 2015, there has been several initiatives to renew a large part of the ferry fleet in Norway by introducing pure battery and hybrid concepts to reduce operational costs and decrease the environmental impacts. Norway is the world leading country in operative and scheduled battery ferries, and by 2021, about 60 battery-powered or hybrid vessels will be in operation [10].

One reason for the opportunity to revolutionize and renewing the ferry fleet is the innovation and cost reduction in lithium - ion batteries. Lithium - ion is today the most common battery technology used in consumer electronics, new electric vehicles and ferries. From Figure 1.1 it can be seen that the cost of lithium-ion batteries has had an exponential decrease the last 8 years, from 8500 NOK per kWh in 2010 to 1500 NOK per kWh in 2018. In the years to come, the cost will be reduced even more with a predicted cost of 1000 NOK per kWh in 2022. Together with the rapid price decrease, the improvements in energy density, that is estimated to increase with 7.5 % every year [20], ensures that the battery is soon to be competitive with a diesel engine in terms of cost and utilization for several more ferry crossings.

A study from Siemens and Bellona states that it is profitable to replace 70 % of the 180 ferries with battery or hybrid solutions in Norway [21]. If this is done, nitrogen
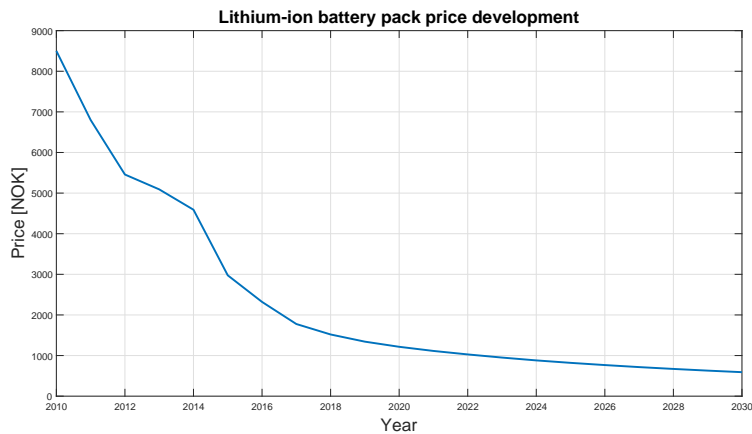
Figure 1.1: Battery cost expectation [8].

oxide (NOx) emissions are cut by 8,000 tonnes per year and CO2 emissions by 300,000 tonnes per year, equivalent to the annual emissions from 150,000 cars [22].

There is little doubt that the new revolution in using zero emission battery ferries will contribute to cleaner fjords and a more sustainable transportation network in Norway. However, this revolution also add new questions, challenges and opportunities that needs to be solved.

Most ferries built have specific characteristics both in terms of design, equipment, operational routes as well as requirements for emission and energy usage. One key problem to investigate is how to smarter plan the charging for such ferries. Optimal charging of battery ferries should take into account many factors such as weather forecast, battery lifetime, available grid power, electricity prices, and power losses. Large costs can be saved if the ferry applies a smarter routine when calculating the requested charging energy per shore docking.

Little is done with regards to smarter charging of battery ferries. However, the car industry has undergone a big change towards using batteries as the mean for operation and much of the research and technology used in this industry are applicable for the battery ferry. Thus, studying some of the work done in the car industry can be of high potential for the ferry industry.

1.2 Objectives

This specialization project will contribute with a study aimed at smarter charging of battery ferries. The focus will be on finding key parameters that influences the charging of a battery ferry and how they can be utilized for more optimal and effective charging. To start, background knowledge about the ferry configuration and operation are needed for building a valid framework. This framework should then be modelled and simulated using a known ferry configuration for operational analysis.

More clearly, the project involves the following objectives:

1. Provide a brief review of the most common battery and hybrid ferry configurations that are used in state-of-the-art new build ferries today.

2. Identify key parameters necessary to plan charging of the ferry more efficient.

3. Identify possible optimization methods suitable for the problem.

4. Develop case study analyses for test and verification of the framework using a known ferry route.

1.3 Assumptions, Limitations & Delimitations

Delimitations are here defined to be boundaries of the study that the writer has control of. Most of the delimitations are related to the system model and simulations and are added for limit the scope of the study.

To not be confused when looking at the simulations and the results, a clear statement will be given here: the model and simulations are based on a ferry operated on only batteries, meaning no diesel generators and other energy sources are influencing the operation. The battery in the ferry is recharged only when docked to the harbour and is discharged only when the ferry is in transit.

The system is based upon ferries operated in Norway and on connections found in the Norwegian transportation network. In the simulations, only one battery ferry is operated in the connection, meaning the charging station at the harbour is only discharged when the same ferry is connecting after crossing the fjord two times.

The battery model is simplified to only consider energy losses due to internal resistance and does not consider capacity fade, temperature increase, power fade and other battery ageing phenomena.

In the power transmission between the local grid, the charging station and the ferry, no transmission losses are taken into account. The active power component is the transferred unit, meaning no reactive power is considered in the model.

In the case study analyses, the system considers weather conditions and electricity pricing as the two parameters for charge planning. The two parameters are not conflicting and are analysed independently. For the weather conditions, only the wind speed is considered to contribute to either load reduction or increase.

Limitations are also present in the model and important to elaborate. The wind model used for the wind speed impact on the ferry is only based on discussions with the supervisors and is not based on any existing verified models. A deviation between the wind load impact on the ferry from the wind model and the actual wind impact on a real ferry must here be taken into account.

Only one data set for the operational profile is used in the simulations. Some modifications are done with this operational profile when considering the weather conditions and when a sensitivity analysis for the electricity pricing is performed. A larger data set, containing several operational profiles could be used to better validate

the results, strengths and limitations with the model.

Some assumptions are done to restrict the scope, and thus necessary to mention. In the simulations of the battery ferry system, it is assumed that the ferry have a predictable operation, keeping the ferry schedule, the charging time limits and that the route is identical for each crossing. The ferry's battery is assumed to be held inside its operational limits, and to always have sufficient energy to cross the fjord.

Another assumption is that grid power is always available to recharge both the charging station and the ferry with the given rated power. The model also assumes that the energy consumption during ferry operation is always predictable, ensuring that the energy transferred to the ferry can be pre-determined.

The battery is assumed to operate predictable, meaning no failures during the simulation period and that the actual power output is the commanded power output. In the transmission system, it is assumed that all equipment have a higher capacity than the power ratings from the battery, meaning that the transmission system can not be a bottleneck to the power transferred.

1.4 Literature Review

Since this report will build up under further work on charging of battery ferries, much work are laid on attaining background knowledge and a bigger overview of the battery ferry operation. Papers on battery systems, power systems and charging strategies are the dominant and most used supportive literature in this report.

Smarter charging of battery ferries is a relatively new term and there is a lack of published work aiming directly at the objectives targeted in this report. Thus, literature on charging strategies and battery systems are mainly related to the automobile industry. It is therefore crucial to gain insight into how such research can be converted into the battery ferry framework and the potential discrepancies which may follow from this.

This literature review aims to provide some insight and discussion on the papers used as a support on the objectives regarding state-of-the-art ferry systems, battery lifetime and charging strategies. First, the review gives a brief overview of the published research regarding hybrid ferry systems and thereby, the review focuses on the literature on battery utilization and lifetime.

Hybrid ferry systems

A presentation of the past, present and future challenges of the marine vessel's electrical power system is given in [23] by E. Skjong. This paper is used extensively throughout the report as a source to both background of battery ferries and shipboard power systems. The paper is a walkthrough of the past development towards the modern ferries that are in use today, and while the paper is not focusing on the charging of battery ferries, it is reflecting upon the forthcoming challenges in power system fault handling and ICT infrastructure among other things.

An approach to economic energy management in diesel - electric marine vessel's is given in [24] by E. Skjong. The paper proposes an optimal EMS algorithm based on a mixed-integer linear programming problem that results in an increase of operational efficiency. While this report will not consider hybrid operation, the paper is used for further understand the load profile and control structure of a hybrid ferry operating on batteries.

The focus in the ferry industry today has been on operating the new battery ferries, dimension the systems and to transfer sufficient energy to meet the load requirements. In [18], DNV GL gives a mapping of the investment needs in the electricity grid for car ferry operation in Norway. The report states that investments above 900 million NOK in the grid are needed to ensure electrification of 52 ferry connections in Norway. Hence, much work and investment are needed for fully revolutionize the car ferry fleet in Norway.

Battery lifetime

Battery life management is a research field with almost unlimited amount of published research papers available. With the increasing development in electric vehicles and smart devices the demand for effective charging strategies for cost savings and battery life prolonging is highly requested.

To achieve effective battery life management, a better understanding of the processes in a battery system is necessary. A review on lithium-ion battery ageing mechanisms and estimations for automobile applications is given in [13] by A. Barré et al., with a presentation of techniques, models and algorithms for battery ageing estimation. The paper also discusses the validity of test bench studies of battery ageing, where the results

often deviates from realistic results due to controlled conditions.

High temperatures for the battery are in [25, 14] reported to have a distinct negative effect on both cycle and calendar life. In [26], a high change in state of charge(ΔSoC) is verified to accelerate the battery power fade. In [27], a high charging current is stated to increase both capacity losses and heat losses. These are just some of the reported variables which effects the battery lifetime and since the variables are not independent of each other, an exact model of battery ageing is hard to develop.

Several attempts on better battery life management are proposed through different types of charging strategies for the battery. Common for all the charging strategies are the conflicting objectives between charging time, energy losses and battery life management. In [28], the optimal charging strategy when considering charging time and energy losses is computed to be the constant current - constant voltage strategy. In [29], a linear quadratic optimization approach for optimally charging a lithium-ion battery, considering charging time, energy losses and temperature rise in the battery, is proposed. However, no results on verified better battery lifetime are presented in the two papers.

In [7, 27], two different charging strategies using a model predictive control (MPC) framework are presented. Both methods are proposing an optimal tradeoff between charging time and battery lifetime and are using two different reduced order models for the battery modelling. Significant improvement in terms of charging time and state of health is observed in [7] and a decrease in both capacity loss and energy loss is observed in [27].

Because of complexity and a large number of variables that impacts on the battery lifetime, a direct connection between battery utilization and lifetime is hard to find. As described in [13], there is currently no study considering ageing as a consequence of all the existent interactions between environment and utilization mode. Thus, obtaining a complete battery diagnosis based on every ageing factor is still a major remaining challenge.

1.5 Background Material & Contributions

As equally important as the results to take with further are the assessments and reflections on the potential for smarter charging of battery ferries presented in this report. The report focuses on enlightening the factors impacting the charging of a battery ferry and to find smarter methods for more effective charging.

The main contributions of this report are:

- Collection of important parameters regarding operation and charging of ferries and the following emphasise on the parameters in the context of smarter charging of battery ferries.

- Proposal of a methodology for controlling the energy transfer with regards to electricity pricing and weather conditions.

Relevant data from actual ferry projects in Norway have been made available by Siemens for this specialization project. The data includes information about the system philosophy of a number of ferries operating in Norway, technical information about battery systems and a realistic operational profile for use in the simulations. The operational profile is generated by BatteryProfileTool, a program developed at Siemens.

The simulink model is made by the writer, but with the battery model being based upon a model given in the course TET4175 - Design and Operation of Smart Grid Power Systems in spring 2018. Two Matlab scripts, given in Appendix B, are used to initialize the parameter values in the Simulink Model.

1.6   Outline

The report is structures as follows: in Chapter 2, the relevant background knowledge on ferry history, power systems and control systems are presented, with an elaboration on battery technologies, types and life management. The two last sections in Chapter 2 involves the system modelling and implementation of the system in Simulink. In Chapter 3, a discussion on charging strategies is given. The constant current - constant voltage charging strategy is presented and a method containing a model predictive controller is proposed.

In Chapter 4, the simulations and results of two study cases are given and compared up against a reference system. The first study case proposes a controller which takes the weather conditions into account and the second study case proposes a controller which considers the electricity pricing. Finally, in Chapter 5, the work done in the project is concluded and a few thoughts on future work are given.

Chapter 2

Methods and Modelling

This chapter will present some background knowledge of battery ferries, their history and how they are configured. Different types of shipboard power systems will be illustrated, and the benefits and disadvantages with AC and DC distribution will be discussed.

For further understanding of the charging strategies given later in the report, a detailed presentation of the lithium-ion battery is given, with comparison to other types of batteries. Benefits and disadvantages are elaborated and how to operate the battery is discussed.

Finally, the system used in the simulations, with its specifications and characteristics, are presented.

2.1   Battery Ferries

A battery ferry is a fully electric marine vessel that can be powered by batteries in all parts of operation. The ferry utilizes a battery energy storage system (BESS) that delivers the power necessary for the propulsion motors and the other critical and non-critical loads onboard during operation. A brief walkthrough of the history towards the development of the first fully electric car battery ferry is given below, and is based on the work by E. Skjong et al. in [23].

The first recorded effort to apply electric power on a marine vessel occurred in the late 1830s after Moritz Hermann Jacobi of Germany invented a simple battery - powered DC motor which was installed experimentally on small boats. In 1880s, the first commercially available shipboard electrical system was built, with the onboard DC system in SS Columbia.

With its 11 meters long and 2 meters wide construction, Elektra, built by Siemens & Halske in 1885, was the first successful electrical powered vessel, powered by a 4.5 kW motor supplied by batteries. A picture of Elektra is given in Figure 2.1.

Figure 2.1: Picture of Elektra. Taken from [9].

An arms race with new technological breakthroughs in electric propulsion and diesel - electric power systems followed in the World Wars I and II, where the development and use of the AC motor and the transformer were central.

The advances in semiconductor technology after World War II revolutionized the field of electronics, and today's modern electric ships takes extensively use of power

electronics to control and convert the electrical energy. The use of power electronics to maximize fuel efficiency became a trend in the 1980s, and applications such as the dynamic position system (DPS) rely heavily on this technology.

In late 2012, the world first hybrid car ferry MV Hallaig was launched. The ferry, built at Fergusons shipyard with support of more than £20 million from the Scottish government, is powered by a hybrid combination of lithium-ion batteries and a small diesel engine. MV Hallaig marked the start for a more environmental friendly ferry configuration, which is the norm in new build contracts today[30].

The recent development in more efficient batteries and energy storage systems has made it possible to build marine vessels operated by only renewable energy sources. In January 2015, the world's first fully electric passenger and car ferry, MF Ampere, was commissioned. The ferry has an installed battery capacity of 1040 kWh, two electric motors of 450 kW and is capable of transporting 360 passengers and 120 cars between Oppedal and Lavik in Sognefjorden.

A modern type of a battery ferry system is illustrated in Figure 2.2. The system is highly influenced by information and communication technology and uses this to control the ferry and the charging process more effectively. The ferry is communicating its states with the charging station at harbour and can remotely command the charging plug to prepare for charging before arriving to optimize the charging period.
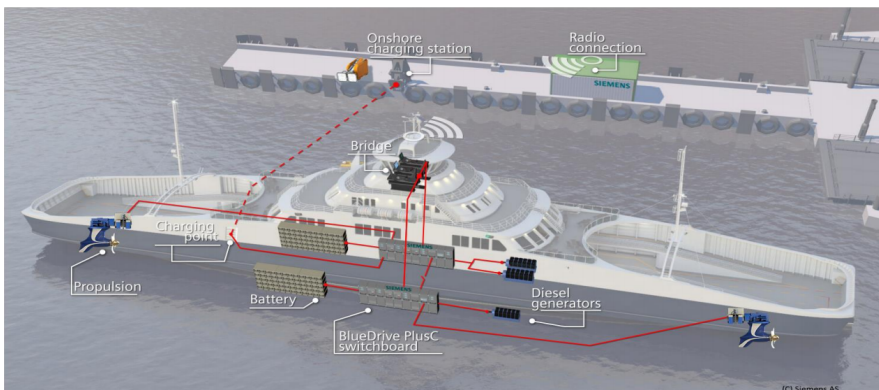
Figure 2.2: Picture of a modern battery ferry system. Taken from [9].

Today's battery ferries have a capacity large enough to operate purely on battery power in routes where the crossing time is less than 30 minutes. For longer operation, the ferry needs support from other power sources, where the diesel engine is most common. Based on the report, [18], from DNV GL, 52 of Norway's ferry routes can be operated by battery ferries where the crossing time of 30 minutes holds and the weather conditions are not to challenging. This calculation is based on a ferry with a car capacity of 120, a crossing speed of 12 knots and the requirement that the ferry should manage to be fast charged within 5 minutes at quay.

2.2 Ferry Power Systems

This section will provide a brief overview of the most common power system configurations used in battery ferries today. The configurations have much in common with the land based distribution system, where energy sources are combined and power is distributed from an electrical substation to small and large loads.

Necessary to mention is that vessels categorized as a battery ferry are typically vessels with a hybrid power system consisting of BESSs and diesel generators. However, the operation is mainly based on only using the batteries as the energy source. Diesel generators are necessary components in a battery ferry with regards to reliability and secure operation, and is typically used when the ferry is operating outside of the normal route and when travelling to or from the shipyard.

The following theory around IPS and PEBBs are based on the work by E. Skjong et al. in [23], and a further discussion on the topics can be found in this paper.

Common for all the configurations is that they are structured as an Integrated Power System (IPS). In an IPS, as shown in Figure 2.3, all the required power, for the vessel's propulsion and service loads, is generated and distributed by the same main energy sources. The IPS shares all power from the energy sources on an integrated power grid, which distributes the power to all individual consumer systems located throughout the grid in a utility fashion. The property of power sharing is the main advantage of IPS and improves power flexibility and availability.

Power electronic building blocks (PEBBs) are important and heavily used components in modern shipboard power systems. Their main objectives is to supply the right form and level of power to the connected systems and equipments. An important power
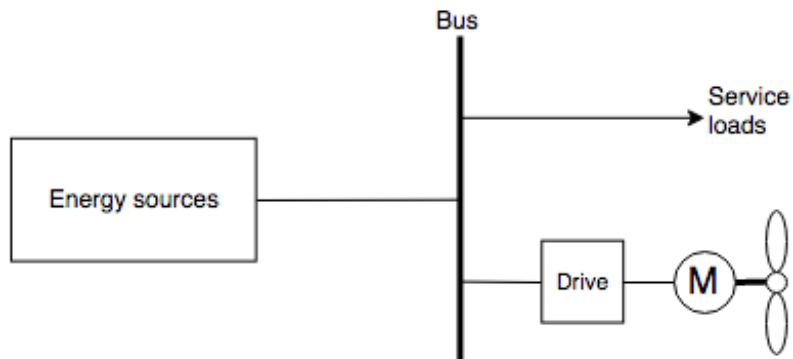
Figure 2.3: Structure of an Integrated Power System (IPS)

electronic device is the voltage source converter (VSC), which is able to convert the electric power from one form to another (AC/DC, AC/AC, DC/AC, DC/DC). The VSC can be programmed to produce voltage and current waveforms, different power factors, and obtain a desired frequency from a range of different input waveforms. The VSC are used in motor drives, active power filters and inverter systems.

The shipboard power system is typically designed to be redundant, where a forward and aft (rear) power station can be operated independently. This requires also redundancy in power system components, making the system more complex but with higher reliability and safety benefits.

2.2.1 AC- and DC Distribution

As described in [23], properties (and requirements) such as reliability, survivability, and continuity of electrical power supply, sustainability, and efficiency can all be related to the power system's design. In the following, the two topologies used in shipboard power systems today - the DC distribution and the AC distribution - are presented.

The characteristics and key points of the two distributions are based on the work by E. Skjong et al. in [23]. The figures illustrating the topologies of the distributions are based on lecture [31] in the course TTK 24 Control of Marine Power Conversion Systems by J. A. Suul, fall 2018.

2.2.1.1   AC Distribution

An AC - distribution power system can be compared to the land-based power distribution in a small township. The bus where the power sources are connected works like the township substation, from where the power is distributed to all users via multiple feeders going to various parts of the township [32]. The AC distribution has the advantage of transforming the power from one voltage level to another without the use of power electronics and fitting in with already AC running devices.

Figure 2.4 shows how a modern type of AC distribution is structured. With today's requirement for flexibility, a DC bus is added to the power system such that loads can be interfaced to both the AC or DC bus. The DC bus is connected to the AC bus through a VSC and a transformer. The system can be compared to a land-based Smart Grid system, where both electrical producers, consumers and storage systems are connected together. The energy storage system (ESS) is connected to a constant voltage DC bus through VSC which controls the power flow to and from the ESS. The ESS can both deliver energy and store the excess energy in the system.

The diesel generators connected in parallel must match the frequency, voltage and phase before connecting to the common AC bus. When matched, the frequency droop lines of the generators determine their share of the total load in the system. Load sharing is controlled by adjusting the prime mover's governor setting, which controls the input valve of the fuel. The governor's automatic control system varies the fuel input rate and the speed directly proportional to the load. When the load increases, the fuel is increased, and vice versa[32].

A back-to-back VSC can be used as a drive system to control the power and speed of the propulsion motor. The back-to-back VSC consists of a converter interfacing the AC bus, a DC link and an inverter interfacing the motor.

As seen, this system design with a hybrid AC - DC distribution depends heavily on the use of power electronics to control power flow and convert the voltage form, making the system more complex.

Compared to the DC distribution system that is presented in Section 2.2.1.2, the AC distribution system has a higher loss of power in the transmission. One reason for this is the skin effect, which due to self-inductance is causing the current to flow on the surface of the conductor and prevents it to flow inside[33]. Another reason is the reactive current component, which reduces the energy transmission capability.
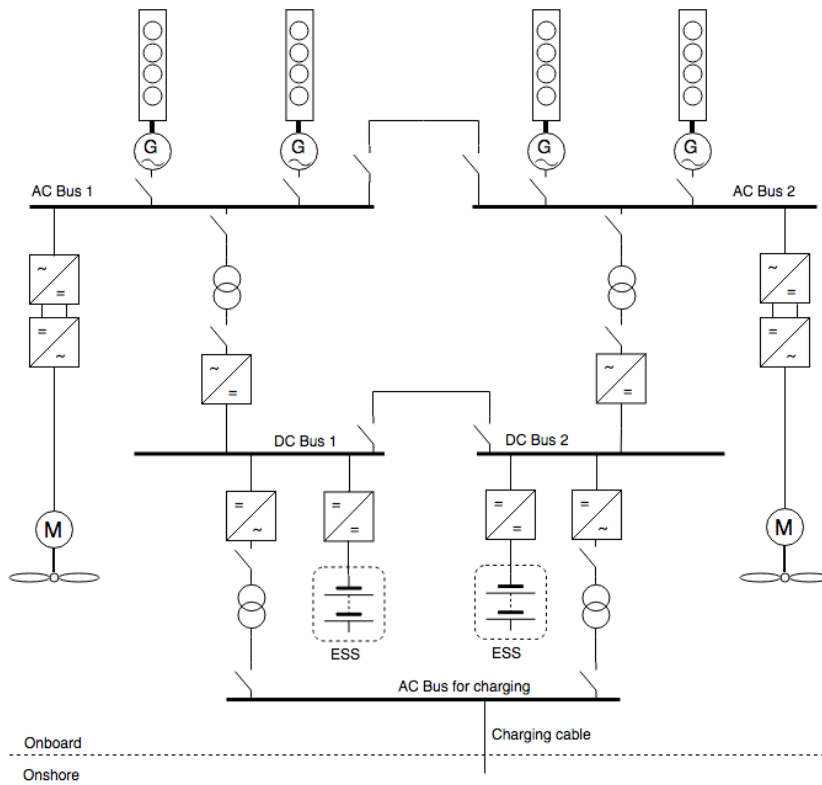
Figure 2.4: Hybrid AC-DC distribution system

A positive side of the AC distribution system is that the impedance in the cables, together with generator- and transformer impedance, limits the short circuit currents. On the other side, impedance of the cables causes a current dependent voltage drop along the cable[34].

If the batteries are used as the main source of energy in the system, it can be more suitable to connect the propulsion system directly to the DC bus. By doing this, the power from the batteries no longer have to flow through the VSC and the transformer to the drive system, which increases the efficiency grade. A power system like this is usually called a DC distribution system, and is described in the following section.

2.2.1.2   DC Distribution

DC distribution systems offers a highly efficient distribution of electric energy by eliminating components for energy conversion and optimizing the use of cables [34]. One example of a DC distribution system is given in Figure 2.5. Here, the propulsion systems, the BESSs and the diesel generators are connected directly to the DC bus through VSCs. An inverter and a transformer is connecting the nominal 1000 V DC bus to the 230 V AC bus, where the charging cable and the other AC utilities are connected.

There are several benefits by using a DC distribution power system. Since frequency control is not a concern at the DC bus connecting the diesel generators, the prime movers can be operated at optimized speed, and thus increasing fuel efficiency. In this power system, voltage droop control, and not speed frequency control, is used to achieve load sharing. By setting different values for voltage droop control for different power sources in a DC system the power ripple can be split over the power sources[35]. Power from the generators can be controlled by adjusting the exciter current in the generator system.

Since phase matching of paralleled power sources is not needed in a DC distribution system, faster power generation response time can be achieved. In addition, since the DC network only requires two conductors for power transmission and that reduction gears in the generator system is not needed for frequency control, weight and space are saved.
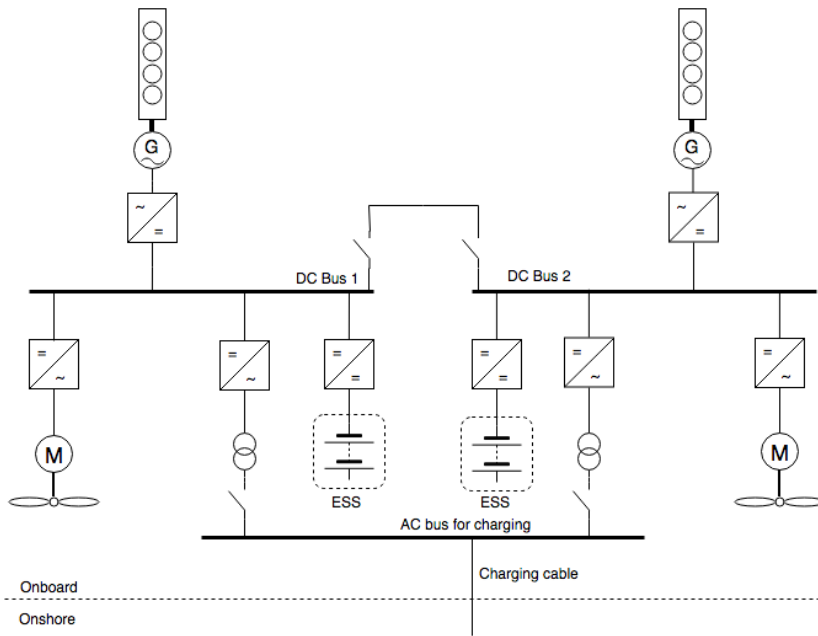
Figure 2.5: DC-distribution system

The DC current does not experience skin effect during power transmission and does not transport reactive current as in the AC network. Thus, the current amplitude is reduced, resulting in lower transmission losses. A consequence of no reactive current flowing in the network is that only the very low ohmic resistance of the cables limits the short circuit currents. This causes a very high short circuit current that equally effects all parts of the power system, which ultimately may damage the system components[36]. A solution, used on modern ships with DC distribution today, is to use solid state bus ties with IGBT transistors as the protection circuits for limit the current rise when a DC short circuit appears.

Comparing the DC distribution in Figure 2.5 to the AC distribution in Figure 2.4, the DC system can be seen as less complex than the AC system. Fewer PEBBs are necessary for a fully functional DC system, and the implementation of ESS is simpler. Since the drive system for the motor propulsion is connected directly to the DC bus, there is no need for a converter, making the VSC less complex.

The complexity could be reduced even more by removing the VSC from the ESS and letting the DC bus voltage float. This would require the VSC connecting the diesel generator to control the DC side voltage to the varying voltage amplitude at the DC bus. If a passive rectifier is used instead of a VSC between the generator and the bus, excitation voltage control can used to control the voltage output to correct value. In addition, if the DC bus voltage is floating and the bus tie between the DC busses are closed, the control objectives of the other VSCs must be changes so that they do not interfere with each other. Two VSCs trying to control the same voltage with a PI-regulator would not perform very well.

Two ferries with different configurations are presented in the following sections.

2.2.2 MF Ampere

MF Ampere, pictured in Figure 2.6, is a car ferry that is operated between Lavik and Oppedal in Sognefjorden in Norway. The ferry is the world's first all-electrical car ferry operated on batteries and is built by the shipbuilder Fjellstrand in cooperation with Siemens and Norled[1].

Figure 2.6: MF Ampere. Photo by Carina Johansen/Bloomberg[10].

MF Ampere is crossing the fjord 34 times a day, with each trip taking around 20 minutes. The ferry specifications are given in Table 2.1. Special for this ferry system is that a battery pack of 390 kWh is installed at each pier to serve as a buffer and to supply electricity to the ferry while it charges. This battery buffer prevents the local grid to be overloaded and it is slowly recharged when the ferry is in transit.

MF Ampere has a simple power system topology, as seen in Figure 2.7. The propulsion motors and the other heavy loads, such as hydraulic power units and the car deck system, are connected to the DC bus together with the ESS. Since the ESS is connected directly to the DC bus without a VSC, the DC bus voltage is floating. Note that the

Table 2.1: MF Ampere specifications. Data from [1, 2]

Length	80 m
Breadth	20 m
Passengers	360
Cars	120
Main engines	2 x 450 kW
Battery capacity	2 x 520 kWh

bus ties are normally operated open and that closed bus ties require considerations regarding the control structure, as discussed in Section 2.2.1.2.

A 230 V / 50 Hz AC bus is connected to the DC bus on both sides of the bus tie through a transformer and a VSC. The auxiliary loads, such as consumer electronics and other equipment are connected to the AC bus. Since there is no generator in the system that is producing a frequency on the AC bus to synchronize to, the EMS must provide a fixed frequency with frequency droop- and load sharing control.
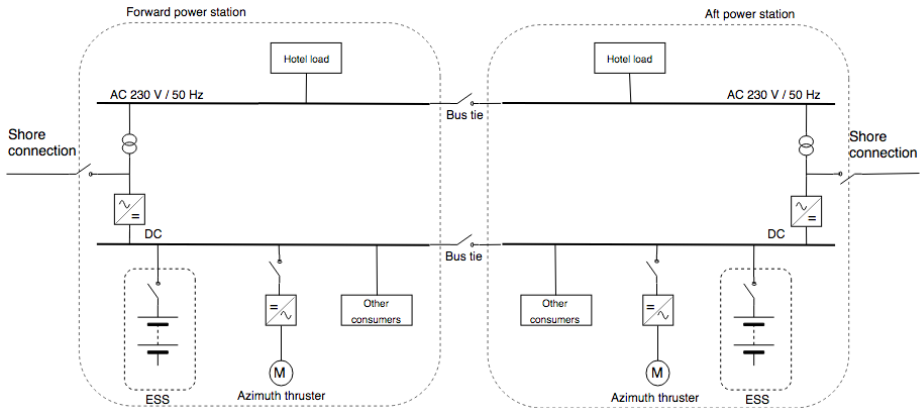
Figure 2.7: Simplified Single Line Diagram of MF Ampere. Based on [2]

Because of reliability and security, the ferry has a separate emergency switchboard used to power emergency equipment in case of a blackout or a fire. The switchboard, not shown in Figure 2.7, have an emergency diesel generator and will supply power to the emergency lightning, car deck system, fire pump and other equipment when needed. The emergency generator can also be used for range extension, which may be needed in situations as when the ferry is moving from or to the yard.

2.2.3 MF Gloppefjord

MF Gloppefjord, pictured in Figure 2.8, is a car ferry that is operated between Anda and Lote in Sogn og Fjordane in Norway. The ferry is a hybrid car ferry with batteries as the main energy source and diesel generators as reserve. The ferry is built by the shipbuilder Tersan in cooperation with Siemens.

Figure 2.8: MF Gloppefjord. Picture from [3]

The crossing time between Anda and Lote is around 10 minutes, and the charging time at each quay is in the range from 5 minutes to 9 minutes. The ferry specifications are listed in Table 2.2.

The single line diagram of the ferry configuration is given in Figure 2.9. The configuration is similar to MF Ampere, but with additional diesel generators connected to the AC bus.

Table 2.2: MF Gloppefjord specifications. Data from [3, 4, 5]

Length	106.2 m
Breadth	16.8 m
Passengers	349
Cars	110
Diesel engines	2 x 550 kVA
Azimuth thrusters	2 x 1200 kW
Battery capacity	2 x 520 kWh
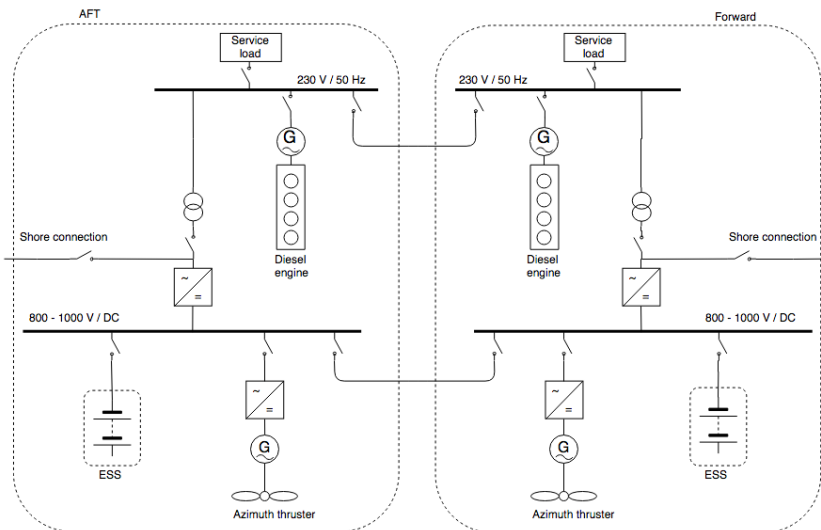
Figure 2.9: Simplified Single Line Diagram of MF Gloppefjord. Based on [5]

With this configuration, the control structure must be based on different operational scenarios. Using only the batteries as the energy source, with the generators turned off, is the most common operational scenario. In this scenario the control structure is identical to MF Ampere, described in Section 2.2.2. When the diesel generators are contributing to hybrid operation, the generators are also producing a frequency at the AC bus, which the VSCs connected to the DC bus needs to be synchronized to.

2.3   Ferry Control System

The control system has a vital part in the overall operation of a ferry. Ferry manoeuvring, power and energy management, alarms and instrumentation are important control mechanisms implemented in a modern ferry. The control system described in this section consists of three parts, with the energy management system (EMS) being the unit in which all other parts are connected to. One part is considering the charging station on shore, another part is considering the power and energy management onboard the ferry and the last part is considering the manoeuvring and control of the ferry.

An illustration of the topology of the ferry's control system is given in Figure 2.10. As seen, the link between the EMS in the ferry and the ESS on shore is wireless and the link between the EMS and the RCS in the ferry is wired.
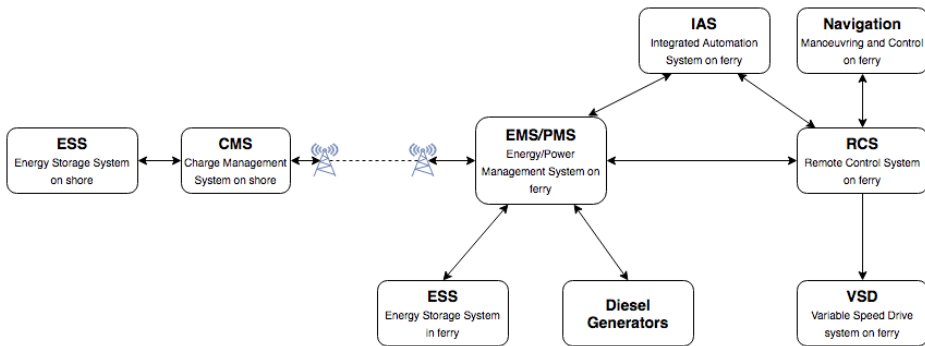
Figure 2.10: Topology of a ferry's control system hierarchy

As described in [24] by E. Skjong, the overall objective of the power and energy management system (PMS/EMS) is to supply the load demand, thus ensuring that all online consumers, and especially consumers that are critical for a given operation experience a stable and reliable supply of power.

The EMS controls the energy to and from the battery and the starting and stopping of the diesel generators. When the ferry is charging at the harbours, the EMS controls the charging power transferred to the ferry and signals the charging station on when to initialize charging and when to stop charging. A charge management system (CMS) in both the EMS and in the charging station is handling the communication between the ferry and the charging station. The communication is going through a wireless link and

radio waves, 4G mobile internet and other communication protocols could be used as a medium for this link.

The Power Management System (PMS) is in charge of balancing the production and consumption, and to make sure that the electrical system is safe and efficient. The PMS is highly integrated with the EMS, and the main difference between PMS and EMS is that the PMS controls the vessel's power plant at instantaneous time with the purpose of stabilizing voltage and frequency and meet load demands, while the EMS often considers events in past and present along with future predictions and estimates [24]. In an industry and sales perspective, these terms have in practice no separation and the EMS is doing all the power and energy management in the ferry.

The Remote Control System (RCS) is controlling the propulsion and thrust units in the ferry. The RCS interfaces with navigation system, which includes the dynamic position system, the joystick and the autopilot among other things. Both the RCS and the navigation system are typically placed on the bridge. When the RCS receives a manoeuvring command, it communicates with the EMS to provide the necessary power and with the variable speed drive system (VSD) to actuate the commanded action.

All systems are connected to an integrated automation system (IAS). This system is monitoring all process values of interest and alarms the operators when an abnormal situation occur.

In addition to the control systems mentioned above, there are supplementary safety control systems for load limitation and overload protection of the battery systems and propulsion systems. Big load transients can occur when the ferry is operating in heavy sea conditions, which may then lead to very high battery currents from the ESS to the propulsion drive system. Protection systems are thus crucial for preventing damage to the battery and the other electronic equipments.

2.4   Battery Technology

Since the battery plays an important part in the battery ferry and for the charging strategies, some background knowledge of the key factors regarding the technology are necessary to obtain. A battery is an electrochemical system that can store electric power by transforming chemical energy to electricity. The battery is used extensively and in a wide variety of applications today, raging from consumer products to industrial plants.

There are two types of electrochemical batteries: Primary batteries and secondary batteries. As described in [32] by M. Patel, the primary battery converts chemical energy into electrical energy, in which the electrochemical reaction is non-reversible, while the secondary battery have a reaction that can be reversed by injecting a direct current from an external source. Therefore, the secondary battery is also known as a rechargeable battery.

Generally, primary batteries have a higher capacity, cost less and have a higher initial voltage than secondary batteries. Typical applications for primary batteries are toys and watches, but the batteries are also used in medical equipments, weapon systems and missiles [37]. Secondary batteries have the advantage of being more cost-efficient over the long term for high utilization applications, but suffers from higher discharge rates and varying battery life ratings. The secondary batteries are used in power tools, computers, electric transportation systems and in spacecraft among other things[38]. To further understand concepts and terms related to the battery, short explanations of key performance characteristics are given in Table 2.3.

Table 2.3: Key performance characteristics in batteries

Characteristic	Explanation
Depth of Discharge (DoD)	Indicates how deeply the battery is discharged.
State of Charge (SoC)	Indicates how much capacity remaining in the battery. The inverse of DoD.
Round Trip Efficiency (RTE)	Defined as the ratio between energy output and energy input at the terminal. Shows how much of the energy that is wasted (turned into heat) in a round trip of full discharge and then full charge[32].
Self-Discharge Rate	A measure of how quickly a cell will lose its energy without any connection between the electrodes due to unwanted chemical actions within the cell[39].
C-rate	Describes how fast the battery will be fully charged or discharged. 1C is equivalent to nominal battery capacity divided by 1 hour.
State of Health	Describes how much the battery capacity is reduced.

In the rest of the section, the secondary battery will be considered since this is the battery type used in hybrid ferries today.

Lead-acid, Nickel-metal hydride and Lithium-ion are some of the rechargeable battery technologies that have been fully developed and are in use in the industrial and consumer markets today. Table 2.4 gives a brief overview of the important characteristics, advantages and disadvantages of the three battery technologies. The data in the table are based on specifications from [32, 40, 41, 42].

Table 2.4: Overview of battery characteristics

Electrochemistry	Typical Applications	Cell Voltage [V]	Advantages	Disadvantages
Lead - acid	UPS, automotive, industry	2.0	Low cost, reliable, robust, can deliver high currents	Heavy, not suitable for fast charging
Nickel-metal hydride	Low cost consumer applications, automotives	1.2	High energy density, low internal impedance, rapid charge, can be deep cycled	High self discharge rate, temperature sensitive
Lithium-ion	Low cost consumer applications, electric transportation, Smart Grid	3.6	High cell voltage, very high energy density, safe, contains no metallic lithium, Low weight, high discharge rate, fast charge possible	Degrades at high temperatures and high DoD, complex measuring of SoC

As seen in Table 2.4, the lithium - ion battery has some nice properties that sets the technology in first position to be used in high power battery applications. Because of this and the fact that lithium ion batteries are used in state-of-art hybrid ferries, the focus hereafter will be on the lithium-ion technology.

2.4.1   The Lithium - Ion Battery

As described in [43] by S. Bashash et al., lithium-ion batteries store electric energy
by shuffling lithium ions between low and high potential energy states via a set of
electrochemical processes. Lithium ions have the lowest energy when they are in the
positive electrode (cathode) and the highest energy when they are in the negative
electrode (anode). During charging, external current forces lithium ions to move from
the cathode to the anode. During discharge, ions naturally move from the anode to the
cathode, creating a useful current. This movement of ions is illustrated in Figure 2.11.
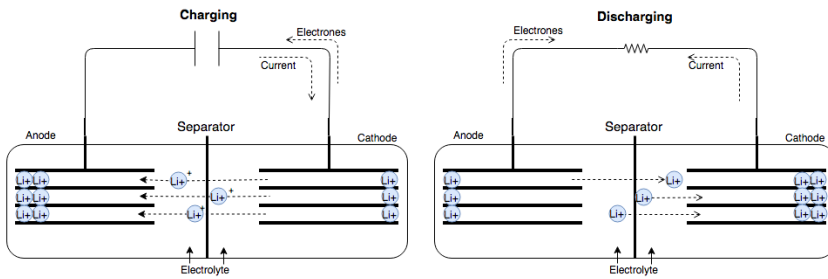
Figure 2.11: Charging and discharging mechanism in lithium-ion batteries. Based on
[11].

In the lithium-ion battery family, there are many different types of cell chemistries.
In this report, the Lithium Nickel Manganese Cobalt Oxide ($LiNiMnCoO_2$ or NMC)
type will be presented, since this is the type used in battery ferries related to Siemens.
The NMC battery is one of the most successful lithium-ion systems, with good overall
performance. Because of their high energy density availability, their zero emission
characteristic during operation and their rather low carbon footprint the NMC batteries
are attractive for use in electrical and hybrid transportation[14].

The key characteristics of this battery type are given in Table 2.5 and are based
on data from [44, 32, 8]. Note that because of the rapid improvement of this battery
technology, some of the specifications can already be outdated.

Table 2.5: Characteristics of NMC battery type

Characteristic	Value	Unit
Voltage (Nominal)	∼ 3.65	V
Voltage (Operating range)	3.0 - 4.2	V
Specific energy (Capacity)	150 - 220	Wh / kg
Charge (Preferred)	0.7 - 1	C - rate
Discharge (Preferred)	1 - 2	C - rate
Temperature (op. range)	+10 to 45	°C
Heat capacity	0.38	Wh / kg·K
Cycle life (Full discharge)	1500 - 3000	Cycles
Calendar life	8 - 10	Years
Self-discharge (at 25°C)	5 - 10	% per month
Cost	∼ 180	$ per kWh

2.4.2   Electrical Circuit Model

The battery can be modelled in many different ways, and dependent on the level of accuracy, the models are ranging from electrical circuits, to simplified electrochemical models and to more complex neural network models [45]. The electrical circuit model of a battery in steady-state is presented in this section and is mainly based on the battery model and theory described in [32] by M. Patel.

As a first approximation, the battery can be modelled with an internal voltage source, V_i, behind a small internal resistance, R_i, as shown in Figure 2.12. With the parameters in Table 2.6, the variation in internal voltage and internal resistance is given by

$$V_i = V_0 - K_1 \cdot DoD$$
$$R_i = R_0 + K_2 \cdot DoD$$

(2.1)

where,

$$\text{DoD} = \frac{\text{Ah drained from battery}}{\text{Rated Ah capacity}}$$

(2.2)

and

$$\text{SoC} = \frac{\text{Ah remaining in battery}}{\text{Rated Ah capacity}} = 1 - DoD.$$

(2.3)

Thus, the internal voltage and resistance vary with the degree of which a battery is discharged. When $DoD > 0$, V_i is lower than V_0 and R_i is higher than R_0.

Table 2.6: Electrical model parameter definitions

Parameter	Definition
V_i	Open - circuit voltage
R_i	Internal resistance
V_0	Open - circuit voltage at SoC = 1
R_0	Internal resistance at SoC = 1
K_1 and K_2	Curve fitting constants
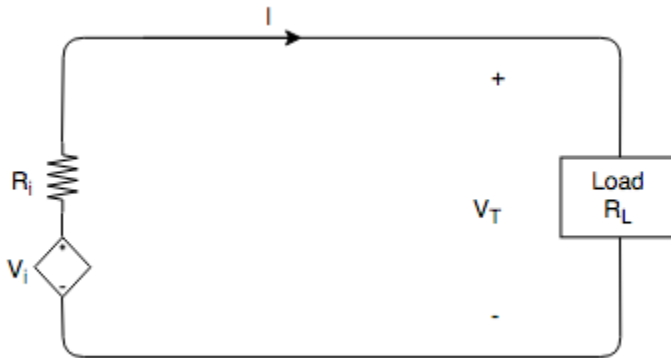
Figure 2.12: Electrical model of battery for steady - state performance

The terminal voltage of a partially discharged battery delivering load current I is less than V_i by the voltage drop over the internal resistance; that is,

$$V_T = V_i - IR_i = V_0 - K_1 \cdot DoD - IR_i.$$ (2.4)

The power delivered to the external load is given by

$$P_{load} = I^2 R_L,$$ (2.5)

where

$$I = \frac{V_i - V_T}{R_i},$$ (2.6)

and the internal power loss in the battery is given by

$$P_{loss} = I^2 R_i,$$ (2.7)

which is dissipated as heat. As the battery is discharged, its internal resistance, R_i, increases, which in turn increases the heat dissipation.

2.4.3 Battery Life

The battery life is an important issue for the implementation of lithium-ion batteries into practical use. Accurate knowledge of lifetime can avoid malfunction and catastrophic failures and ensure stability and safety of the batteries[46].

As defined in [32] by M. Patel, the battery life is measured in number of cycles it can be discharged and recharged before the active electrode material wear out. When the active anode material is exhausted, there will no longer be a current flowing between the anode and cathode. The battery life depends strongly on the electrochemistry, and also on the depth of discharge and temperature as will be further discussed. As an example, Figure 2.13 illustrates the dramatically effect by operating the battery with a high DoD.
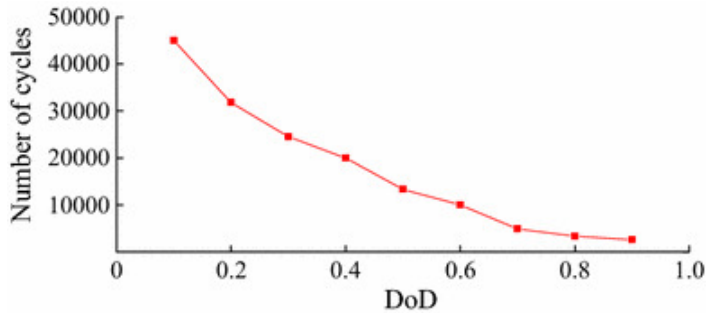
Figure 2.13: Cycle life versus DoD curve for lithium-ion NMC battery. [12]

In the following, some of the ageing and degradation mechanisms in a battery are identified. Identifying the mechanisms is a challenging goal, because battery processes are complicated as many factors from the environment and from utilization interact to generate different ageing effects. The theory on ageing effect is based on [13] by A. Barré et al. which provides a review intended to summarize today's results on mechanisms, factors and estimation methods of lithium-ion battery ageing on automotive applications.

2.4.3.1 Electrochemical Ageing

For every charge cycle, the capacity in the battery will be reduced due to irreversible processes in the battery chemistry. One of this processes is the development of a solid interface on the electrolyte / negative electrode interface, and is named Solid Electrolyte Interphase (SEI). This solid interface is naturally created during the first charge and have the advantage of protect the negative electrode from corrosions and being a barrier between the negative electrode and the electrolyte.

However, when the battery is operated outside its electrochemical stability range, in terms of temperature and utilization, the SEI becomes unstable and develops over time. This induces loss of lithium ions and electrolyte decomposition as the SEI is expanding. Loss of available lithium due to side reactions at the negative electrode has been reported as the main source of ageing during storage periods[25]. With time, there is also a loss of active surface on the negative electrode, increasing the electrode's impedance.

Under high temperatures, the SEI may dissolve and create lithium salts less permeable to the lithium ions and therefore increase the negative electrode impedance. On the contrary, low temperatures can lead to a lithium plating overlay

Figure 2.14: Ageing effect on the negative electrode. Illustration taken from [13]

on the electrode. The SEI formation and development and the lithium plating are all responsible for the loss of cycleable lithium, reducing the battery's capacity over time. Figure 2.14 illustrates the phenomena taking place at the negative electrode.

2.4.3.2   Calendar Ageing

The calendar ageing corresponds to the phenomena and the consequences of battery storage and is the irreversible proportion of lost capacity during storage. The main condition considering the calendar ageing is the storage temperature. Corrosion and lithium loss are more present when the temperature is high, causing capacity fade. The SoC is another factor that contributes to calendar ageing, where a high SoC causes more battery degradation due to higher cell voltage and more tension on the stability limit of the electrochemistry.

Figures 2.15 and 2.16 shows the reduction in battery capacity and charge cycles with regards to the ambient temperature and SoC, respectively. Keeping the ambient temperature around 25°C and the SoC level around 60 % will, as seen from the figures, prolong the battery lifetime.
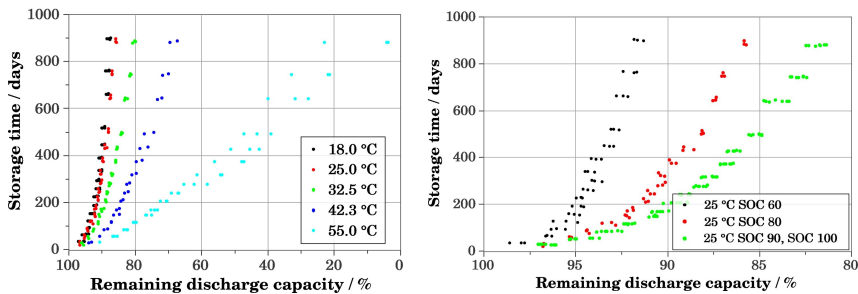
Figure 2.15: Calendar ageing dependent on the temperature. SOC = 80 % [14]

Figure 2.16: Calendar ageing dependent on the SOC[14]

2.4.3.3   Cycle Ageing

Cycle ageing happens when the battery is either in charge or in discharge. The battery's SoC, utilization and temperature conditions are some of the factors that contributes to cycle ageing. Hence, all factors described in Sections 2.4.3.1 and 2.4.3.2 have an impact.

Results from [26] by I. Bloom et al. show loss of battery power as the state of charge variation during a cycle, (ΔSoC), is high. Other factors impacting the cycle ageing are the charge/discharge voltage and current amplitude. A high voltage is causing more tension in the electrochemistry, while a high current is causing an increase in temperature which accelerates the ageing phenomena.
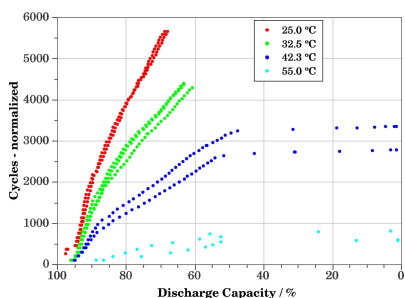
Figure 2.17: Cycle ageing dependent on the ambient temperature. [14]
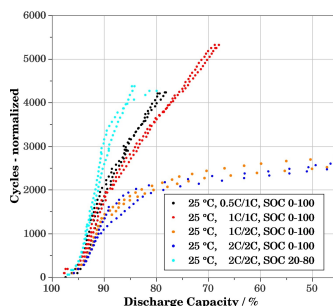
Figure 2.18: Calendar ageing dependent on the C-rate[14]

As seen in Figures 2.17 and 2.18, the ambient battery temperature and the charge and discharge C-rate have a big influence on the battery's SoH. High temperature during utilization decreases charge cycles and SoH rapidly. An interesting observation is that increasing the discharge rate has more negative effect on the SoH compared to increasing the charge rate.

It is essential to have a control on the ambient battery temperature to avoid operating the battery outside the acceptable temperature range. Typical cooling solutions that are used are air or water cooling.

To find an optimal way to operate the battery, covering all the variables stated above, to prolong the battery life is a hard task. To summarize, controlling the current amplitude to limit the temperature increase and keeping a low depth of discharge will have a positive effect on the battery lifetime. Hence, this will be a focus in the charging strategies.

2.5   System Modelling

The system used in the model and simulations in Chapter 4 is described in this section. Each component in the system is presented with its specifications and characteristics, and important assumptions and simplifications that deviates this model from a real system are also discussed.

The system consists of a ferry connected to a charging station and the local grid as illustrated in the topology in Figure 2.19. The ferry configuration consists of an energy storage module, a propulsion load and a hotel load. VSCs are added to the figure to illustrate the voltage form in the system. The level of detail is chosen on the background of the simulation objectives, which are mainly considering power flow between the charging station and the ferry.
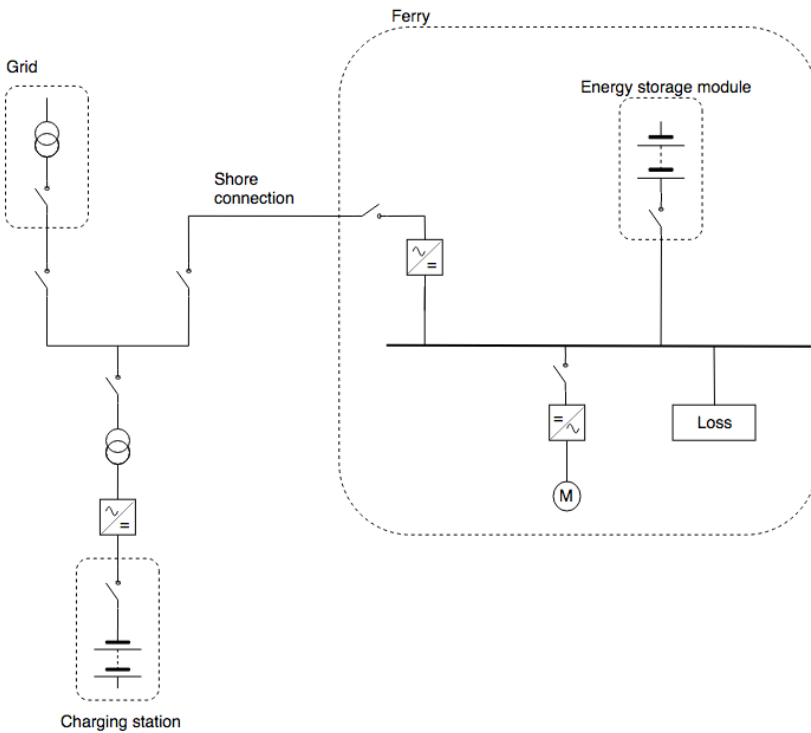
Figure 2.19: System topology

The power flow in the network, from the grid to the charging station and ferry, is defined to be the active power component. Hence, only the useful power and not the reactive power is considered in the simulations. This is an important simplification of the system, since a real ferry would draw a big share of reactive power from the grid.

As seen in the system topology, only one charging station is modelled, whereas in a real system, and in the simulations, the ferry is operated between two charging stations. This is solved in the simulations by ensuring that the battery in the charging station always has been recharged to upper SOC limit before the ferry is connected. In the simulations, the ferry can be in the 7 different operational modes given in Table 2.7.

Table 2.7: Operational modes of ferry

Mode	Description
At Quay	Ferry loading or unloading passengers
Manoeuvring 1	Manoeuvring out of quay area
Acceleration	Increasing speed to transit speed
Transit	In transit
Deceleration	Decreasing speed to manoeuvring speed
Manoeuvring 2	Manoeuvring to the quay area
Connection / Disconnection	Connection or disconnection of charging equipment

2.5.1   The Grid

The power delivered from the grid to the charging station and the ferry is in this model defined to be constant. The rated grid power is given in Table 2.8 and defined to only consist of the active power component.

Table 2.8: Grid Characteristics

Rated Grid Power	1500 kW

When the ferry is charging, the ESS on the ferry is fed with power from both the charging station and the grid. The grid is always delivering the rated power, while the power from the charging station can be controlled and adjusted accordingly to meet specific charging objectives. While the ferry is offshore, the battery in the charging station is charged with the rated grid power to the upper SOC limit. This normally takes 7 minutes after a charging time of 4 minutes.

2.5.2   The Charging Station

The charging station is modelled with an ESS and connections to the local grid and the ferry. The specifications of the ESS in the charging station are listed in Table 2.9.

The battery is designed to be close to a realistic system, with battery modules connected in series and parallel in order to achieve the desired nominal voltage of 930 V and the capacity of 1200 Ah. The ESS in the charging station and the ferry are identical except from the capacity, which is higher in the ferry's battery. Since the ferry demands high performance for the battery to be operated in all conditions, the battery is designed with a high efficiency factor, meaning low internal impedance and low transmission losses.

To prolong the battery lifetime, the battery is operating between an upper and lower SoC limit. This is a strict limit, meaning that the charging will stop at 65 % SOC, and the discharging at 20 % SOC. This operational range is determined on the background of the theory presented in Section 2.4.3.

The charging station and the ferry is communicating its states with each other during operation. This ensures that the controller in the charging station always know

Table 2.9: Specifications for the ESS in the charging station

Battery Type	Lithium - ion (NMC)
Capacity	1200 Ah / ~ 1110 kWh
Effective Capacity	540 Ah
Max Power	4140 kW
Max C - Rating	4452 A
Max Charging Voltage	1053 DC
Efficiency Factor	0.97
SOC Upper Limit	0.65
SOC Lower Limit	0.2
SOC Initial	0.65

the ferry's SoC and can then calculate the amount of energy needed to be delivered before the charging process begins.

A simplification in the charging process is the instant ramp up in power transmission when the ferry starts to charge. In a real situation, the current would ramp up in amplitude for approximately 10 seconds before reaching its maximum charging current. In this model, the current is assumed to ramp up immediately after connection, and the ferry is charged with a constant power during the charging period.

2.5.3 The Ferry

The ferry is modelled with an ESS, a propulsion load and a hotel load. For simplicity, the ferry is modelled without diesel generators. This requires the ESS to have a capacity large enough to deliver the load demand requested in the modelled period. The ferry's ESS specifications are listed in Table 2.10.

A high capacity is chosen such that the ferry is able to operate its route schedule with limited charging time and to have some degree of freedom when deciding the amount of energy transferred to the ferry. The ferry's ESS is else similar to the charging station's ESS.

A controller in the ferry is controlling the ESS to deliver the power necessary to met the load demand. The ferry is following a pre-deterministic operational profile and it is assumed that the ferry is able to always follow the route schedule. During transit, the

Table 2.10: Energy Storage System on Ferry

Battery Type	Lithium - ion (NMC)
Capacity	5200 Ah / ~ 4800 kWh
Effective Capacity	2340 Ah
Max Power	4140 kW
Max C - Rating	4452 A
Max Charging Voltage	1053 DC
Efficiency Factor	97 %
SOC Upper Limit	65 %
SOC Lower Limit	20 %
SOC Initial	65 %

ferry can experience load variations due to weather conditions, which can be turned on and off in the simulations.

The operational profile and load characteristics for the ferry are further discussed in Section 2.5.5.

2.5.4 The Energy Storage System

Both the charging station and the ferry have an energy storage system (ESS). The ESS consists of an energy storage module (ESM) and a power electronics module (PEM), as illustrated in Figure 2.20. The ESM is the unit storing the energy in the system and controller logic, security electronics and other systems to manage the ESS are included in the PEM.
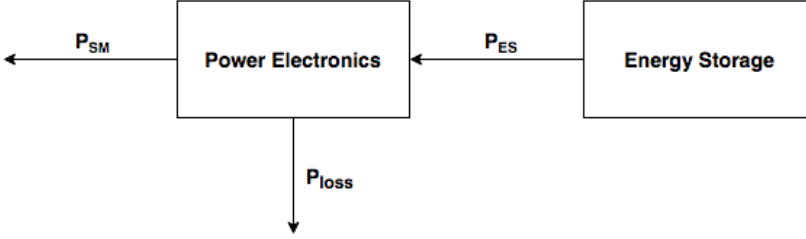
Figure 2.20: Model of Energy Storage System

Power flow in the direction of the arrows indicates discharging of the ESM, and power flow in the opposite direction indicates charging. Hence, when discharging, the useful power going out of the storage medium is $P_{SM} > 0$ and when charging $P_{SM} < 0$. Power losses in the PEM are modelled as a single loss given by

$$P_{loss} = P_{ES} - P_{SM} > 0. \tag{2.8}$$

The power output from the ESS when discharging is given by

$$P_{SM} = \eta P_{ES} > 0 \tag{2.9}$$

where η is the efficiency factor for the ESS. The power loss when discharging is then

$$P_{loss} = \frac{P_{SM}}{\eta} - P_{SM}$$
$$= (\frac{1}{\eta} - 1)P_{SM}. \tag{2.10}$$

When the ESS is charging, the power to the energy storage is given by

$$P_{ES} = \eta P_{SM} < 0, \tag{2.11}$$

and the power loss is then

$$P_{loss} = \eta P_{SM} - P_{SM}$$
$$= (\eta - 1)P_{SM}. \tag{2.12}$$

Note that the efficiency factor is assumed to be the same for charging and discharging the battery. To get a more realistic dynamic of the battery's SoC, the varying terminal voltage of the battery is used to calculate the current. The current in the battery is given by

$$I_{ES} = \frac{P_{ES}}{V_T}, \tag{2.13}$$

where V_T is the terminal voltage of the battery. The terminal voltage dynamic is non-linear and changes with respect to the battery's SoC. When calculating the current, the values from Figure 2.21 are used for the terminal voltage, which are based on data from Siemens battery systems.
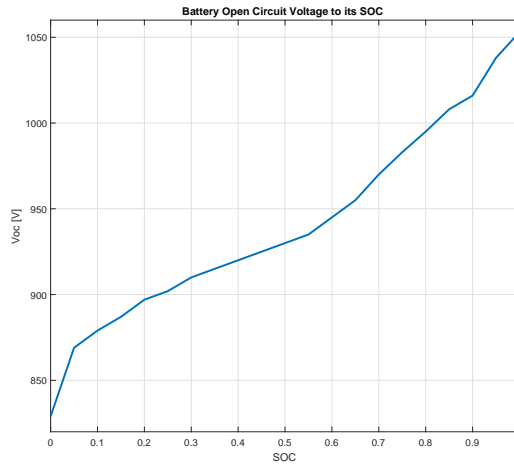
Figure 2.21: Terminal voltage vs. SOC

2.5.5 Operational Characteristics

The operational profile for the model are based on a tool for generating ferry load profiles by Siemens and the schedule for the ferry route between Lavik and Oppedal in Sognefjorden. The route is operated by Norled AS and the route schedule can be found at their website[47].

The operational profile has a duration of 24 hours, starting at 03:00, as seen in Figure 2.22. The ferry starts by being in nightlay until 06:00, when the first crossing takes place. At 06:56, the ferry is back at the first harbour and is docked till 07:30. In this time, the ferry's battery is recharged to its upper SoC limit, as seen by the SoC profile in Figure 2.23.

Normal operation between the two harbours, as given in Tables 2.11 and 2.12, is followed for the rest of the day, with an exception at 10:00, when the ferry is docked for an additional 10 minutes. During this pause, the battery is again recharged to the upper SoC limit.

The SoC profile of the ferry, given in Figure 2.23, shows that the battery is recharged to upper SoC limit two times during the modelled period and that this occurs when the ferry has longer docking periods at 07:00 and 10:00. Under normal operation, the ferry is consuming more energy than it is supplied, and hence, the SoC is decreasing in the period from 10:10 to 23:36. The lowest SoC during the period is 29% which occurs at the end of the last crossing.

After the last crossing, the ferry is immediately switched to nightlay-mode. In this mode, the power consumption in the ferry is constant at 13.5 kW. This load is met by the local grid, which is simultaneously recharging the ferry's battery back to upper SoC limit with a reduced transferred power of 930 kW.

In Figure 2.24 the SoC profile for the battery in the charging station is given. As seen, the battery is never operated outside its SoC limits, and is always recharged to upper SoC limit by the rated grid power when the ferry is in transit. In a real system the battery in the charging station could be recharged more slowly because the ferry has to cross the fjord two times before reconnecting to the same charging station. Hence, in this system, the same charging station is used to look at the dynamic in two stations, at the same time.
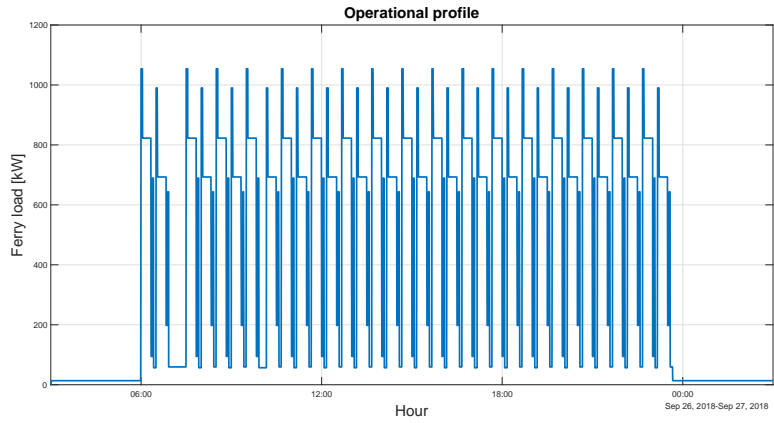
(a) Operational profile of ferry over 1 day
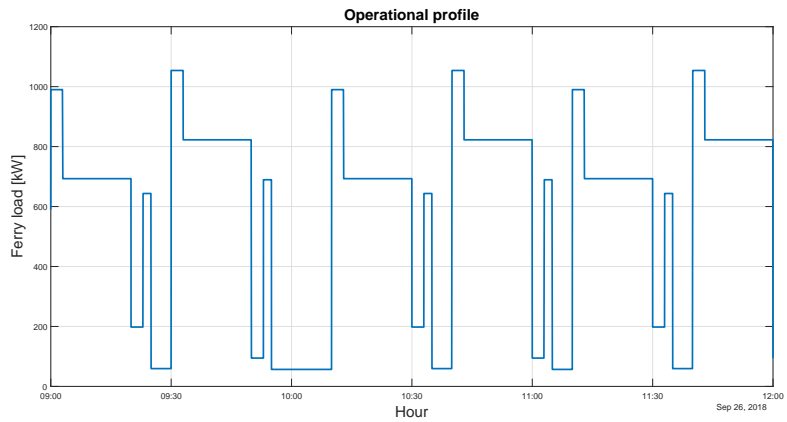
(b) Operational profile of ferry from 09:00 to 12:00

Figure 2.22: Operational profile of ferry
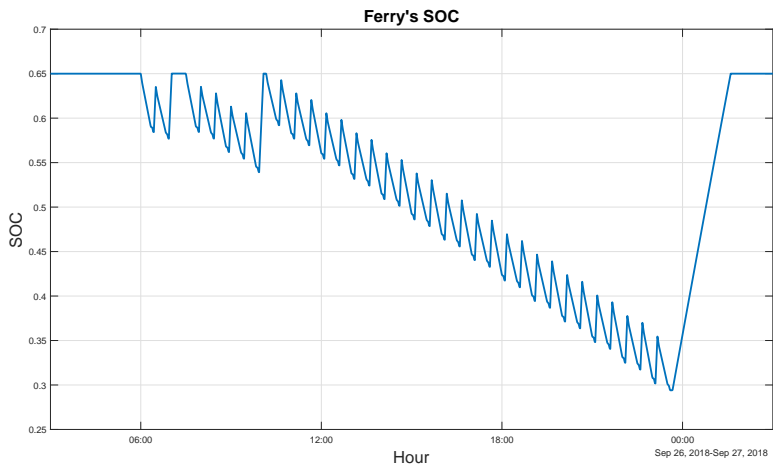
Figure 2.23: Ferry SOC profile
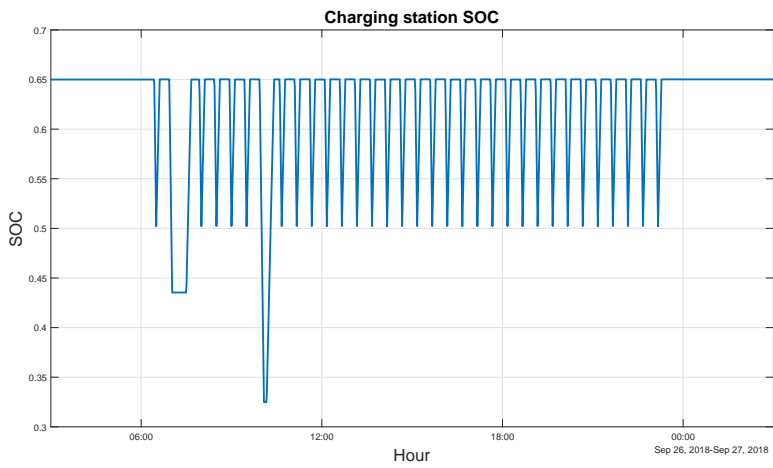
Figure 2.24: Charging station SOC profile

In addition to nightlay, the operational profile is divided into 7 modes. The operational profiles for leg 1 and leg 2, with the power and time used in each mode, are given in Tables 2.11 and 2.12 respectively. The profiles are generated by a tool developed at Siemens.

Table 2.11: Normal operational profile - leg 1

Mode	Power [kW]	Duration per trip [min]
Manoeuvring 1	689.4	0.5
Acceleration	1053.9	2.5
Transit	822.6	17
Deceleration	94.5	3.5
Manoeuvring 2	689.4	1.5
Connection / Disconnection	56.7	1
At Quay	56.7	4
Charging	3929.7	4
Total		30

As seen in the tables, the power used in the modes are different for the two stages, resulting in the ferry using more energy in leg 1 compared to leg 2. To justify this modelling, DNV GL states that energy consumption is dependent on many factors such as the sea surface, shape of the ferry and wave resistance, and that variations can occur internal in the ferry connection[18].

Hotel load is also incorporated in the model. When the ferry is one of the operational modes given above, the hotel load is included in the power used. When the ferry is in nightlay, the hotel load is defined to be 13.5 kW. The local grid is supplying the power necessary to meet this load demand.

In Tables 2.13 and 2.14 the energy budget in respectively leg 1 and 2 are presented. The budgets shows that the ferry uses 12.6% more energy in leg 1 compared to leg 2 and that this results in a more negative balance, and thus making a higher impact on the battery's SoC during leg 1.

Table 2.12: Normal operational profile - leg 2

Mode	Power [kW]	Duration per trip [min]
Manoeuvring 1	643.5	0.5
Acceleration	990	2.5
Transit	693	17
Deceleration	198	3.5
Manoeuvring 2	643.5	1.5
Connection / Disconnection	59.4	1
At Quay	59.4	4
Charging	3929.7	4
Total		30

Table 2.13: Energy budget - leg 1

Mode	Energy [kWh]
Ferry in transit	310.2
Ferry charging	262
Balance	-48.2 kWh

Table 2.14: Energy budget leg 2

Mode	Energy [kWh]
Ferry in transit	275.6
Ferry charging	262
Balance	-13.6 kWh

The charging capacity is in normal operation 90% of full capacity, meaning that maximum charging power is 4322 kW and maximum energy that can be delivered to the ferry in a normal charging time of 4 minutes is 288 kWh. With maximum charging power the energy balance in leg 2 would be positive, meaning that the ferry would receive more energy that it consumes in leg 2. In leg 1, the negative balance would be reduces and overall the ferry would operate on a larger margin to the lower SoC limit.

2.5.6   Weather Characteristics

The weather conditions have an important impact on the ferry. Waves, sea currents, headwind and tailwind are factors that will change the total ferry load and thus, must be considered when determining the capacity of the energy storage.

In this model, only the wind speed and wind direction are added as a factor for the ferry load. The wind profile is given in Figure 2.26 and shows the wind speed at Sandane Airport in Sogn og Fjordane between the 26th and 27th of September 2018. The weather data is retrieved from [6] by yr.no and is presented in detail in Appendix A. Sandane Weather Station is chosen because of the nearby ferry crossing between Anda and Lote, which crosses the fjord in a north - south direction, as seen in Figure 2.25.

It is chosen a windy day with large variations for the wind speed. This is chosen for easier see the impact on the total ferry load and the potential in controlling the transferred energy accordingly to the weather conditions. During the time the ferry is in operation, the wind speed is at its maximum with 11.2 m/s at 08:00, and at its lowest with 1.6 m/s at 21:00. The wind speed is high during the morning and afternoon, and decreases throughout the evening.

Since the ferry is modelled to cross the fjord in a north - south direction, a wind direction from north would effect the ferry as a headwind when the ferry is in transit to the north harbour, and as a tailwind when the ferry is in transit to the south harbour. The vice versa is happing if the wind is coming from the south.

An illustration of this is given in the wind phasor plot in Figure 2.27. As the wind can take intermediate directions between north, south, east and west, the different directions will have different effect on the ferry. γ is chosen to represent the directional factor and can take a value in the range between 0.5 and 1. A negative γ represents a tailwind for the ferry, while a positive γ represents headwind.

Figure 2.25: Map over the ferry crossing between Anda and Lote. From [15].
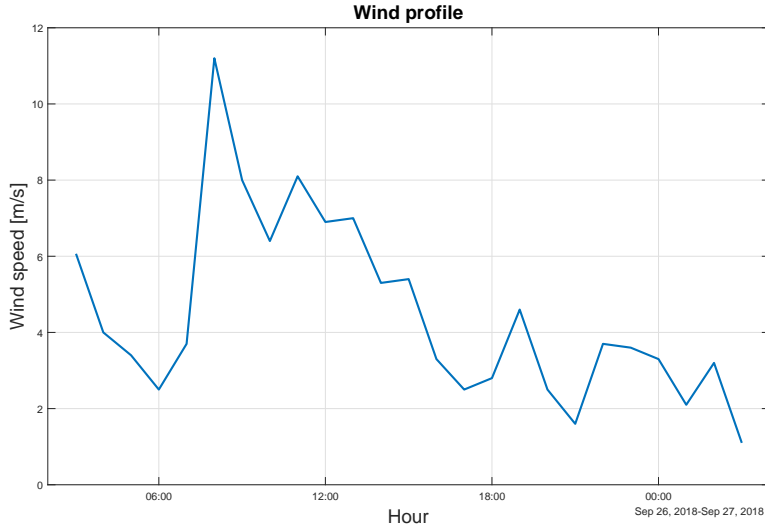
Figure 2.26: Wind profile

In addition to this, it is assumed that the normal load profile, given in Figure 2.22, has an average wind speed of 2.5 m/s already included in the load. A consequence of this is that a wind speed below 2.5 m/s will reverse the situation above, meaning that a tailwind of 0.8 m/s will increase the total load for the ferry.

The wind impact is adjusted accordingly to the operation of the ferry, meaning that when the ferry is in one of the modes with high load demand, the wind impact is also high. Hence, with this wind model, the ferry will experience a higher wind impact when accelerating and in transit, than it will when decelerating and manoeuvring to the quay. The wind power is given by

$$P_{wind} = P_{ferry} \frac{\omega - \omega_{avg}}{\omega_{max} - \omega_{avg}} \cdot \gamma, \tag{2.14}$$

where P_{ferry} is the actual ferry load, ω is the actual wind speed and ω_{avg} is the average wind speed. Hence,

$$\omega_{avg} = 2.5 \text{ m/s.} \tag{2.15}$$
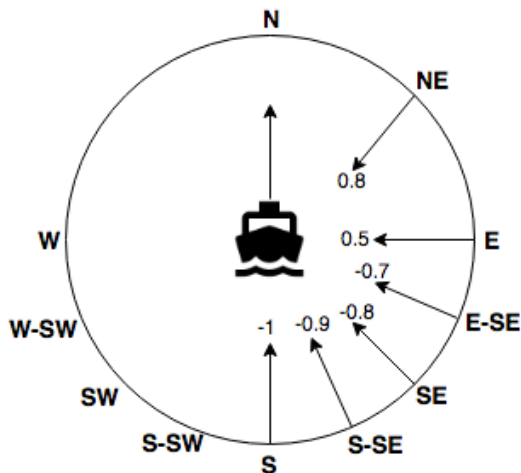
Figure 2.27: Wind phasor. γ is represented by the numbers.

P_{wind} can be both positive or negative regarding on the sign of γ and the value of ω. $\omega = \omega_{avg} = 2.5$ will result in zero effect on the ferry from the wind. In the model, ω_{max} is defined to be 50 m/s, resulting in an increase or decrease of 18% in total ferry load with a wind speed of 11 m/s and a γ equal ±1.

The Ferry's total load and the power that the battery needs to deliver is then given by

$$P_{tot} = P_{ferry} + P_{wind} \tag{2.16}$$

2.5.7   Electricity Price Characteristics

To operate a battery ferry is very power demanding. A huge amount of energy is drawn from the grid to meet the load demand in the charging station and the ferry. Since the electricity price is varying throughout the day, large costs can be saved by better planning the charging of the batteries.

Only the price of electricity is considered in this study, meaning that grid rental and special tariffs are not taken into account. The electricity price dynamic used in the model is given in Figure 2.28. In the figure, a curve representing the normal electricity price from Nordpool's market data[16] in the Molde-region is plotted. The curve is based on the averaged hourly prices over the period from 29th October to 3rd November 2018.

The other curve in Figure 2.28 is representing the adjusted electricity prices. This curve is a scaled version of the normal price curve and is used in the simulations for better see the potential in smarter planning of battery charging.
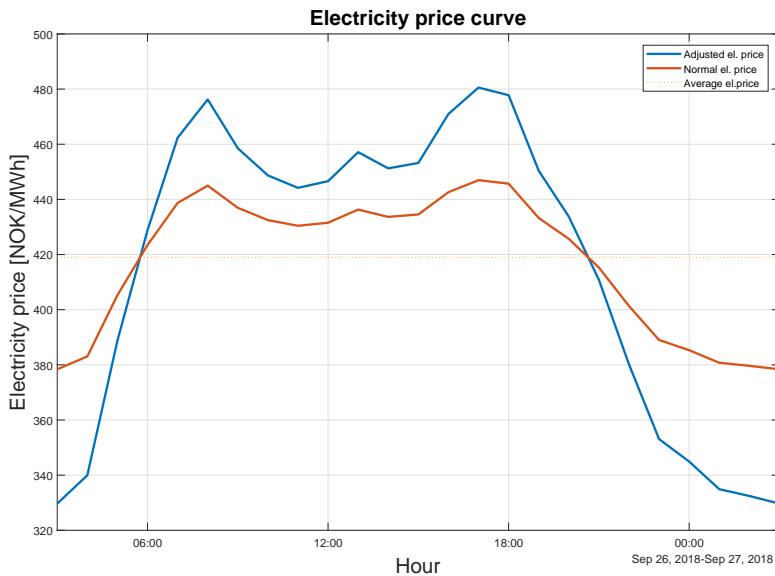
Figure 2.28: Electricity price curve over 1 day[16]

2.5.8 Further Model Considerations

In the model, only one battery ferry is assumed to operate in the ferry connection. Hence, this model is similar to the Lavik-Oppedal connection, where one battery ferry (MF Ampere) is operated together with two other ferries driven by diesel engines. In other ferry connections, such as the Anda-Lote connection, two hybrid ferries, mainly driven on batteries, are operated together. This case would not be suitable for the model, hence a limitation is given here.

A simple model for the ESS is chosen for the system. The ESS in both the charging station and the ferry are assumed to operate ideally, with no failures and battery degradation throughout the simulated period. The power output from the ESS is only constrained by the power ratings for the battery and no thermal or electrochemical factors are considered when operating. Temperature and battery degradation could be estimated by adding more complexity to the ESS model, which could then be further used for better analysing the charging strategies.

A simple model for the grid connection is chosen, with no power variations during the simulated period. In a real system, the available grid power would vary some during the day, and by adding this variation and taking the reactive power component into account, a more realistic model could be obtained.

Important assumptions for the model when considering the simulation results are summarized in the list below:

- Single battery ferry operating in the connection.

- Constant power from the grid. (Except from nightlay)

- Zero transmission losses.

- Predictable energy consumption - Energy consumption can always be predicted before charging process begin, even when considering weather conditions.

- Predictable operation - No discrepancies from the operational modes.

2.6   Simulink Model

The model is built and simulated in Simulink, a graphical programming environment for modelling, simulating and analyzing dynamical systems developed by Mathworks[48]. The solver used is a ODE3 fixed-step solver with a sampling time of 1/60. The resolution of the data is in minutes, meaning that the data set for 1 day contains 1440 data points. The solver interpolates between the data points, resulting in a data set of 86401 points for each variable simulated.

When the model is simulated, it retrieves the system parameter values from a configuration file in Matlab. This configuration file, given in Appendix B, initializes the data time series from the BatteryProfileTool and sets the parameter values before the Simulink model is run.

In the next sections, the most important blocks of the model are presented. The additional blocks are given in Appendix C.

Overall System

The top level of the modelled system is given in Figure 2.29. Here, the three main components in the system, the grid, the charging station and the ferry, are shown together with the connection between them. On the transmission lines there are modelled a reduction gain for the transmission losses. This gain is equal to 1 in this system, meaning that no transmission losses are present in the system.

Since the ferry and charging station are communicating, a signal for the ferry's SoC is going from the ferry block to an input on the charging station block. This is used in the charging station's controller to control the power transferred to the ferry.
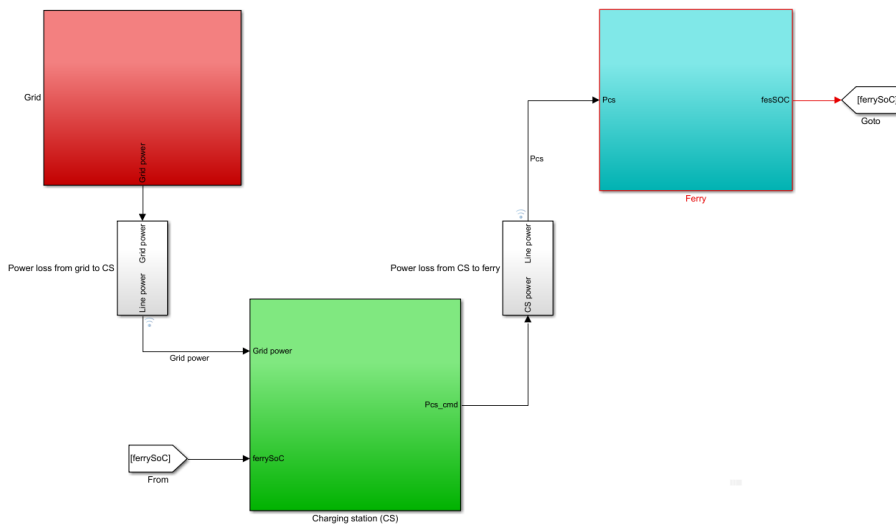
Figure 2.29: Overview of the simulink model

The Grid

The grid block, given in Figure 2.30, is the simplest block in the model, only consisting of the constant rated grid power transferred to the charging station and the ferry. A more complex grid model could be considered, as discussed in Section 2.5.8.
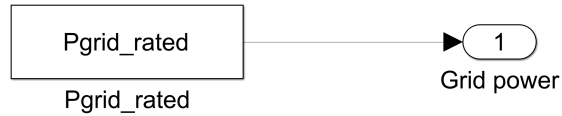
Figure 2.30: The grid modelled in Simulink

The Charging Station

The charging station block consists of an energy storage module and a controller module, as seen in Figure 2.31. When the ferry is charging, the output from the charging station block is the sum of the power from the ESS and the local grid. When the ferry is in transit, the local grid is recharging the battery and the output from the block is zero.
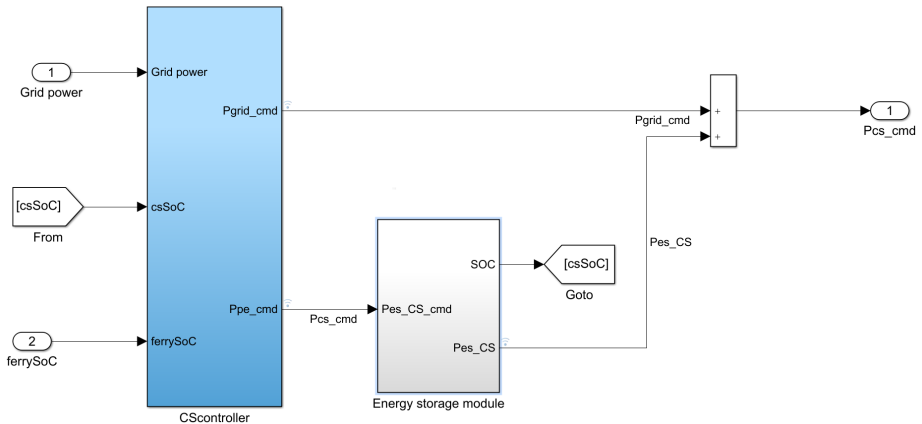
Figure 2.31: The charging station modelled in Simulink

The charging station's controller module, given in Figure 2.32, is the most complex block in the model. The controller's main objective is to control the power to and from the ESS and decide when to transfer power to the ferry. The output of the block is the commanded grid power to the ferry and the commanded ESS power. Note that the commanded ESS power can be both positive and negative, where a positive value commands the battery to discharge, while a negative value commands the battery to charge. Also note that the commanded grid power is always the rated grid power, except from when the ferry is in nightlay.

Logic is implemented in the controller block to switch between the different operational modes of the ferry. The modes and their outputs are describes in the list below.

- Ferry offshore: When the ferry is in transit, zero power is commanded to the ferry. The controller commands the battery in the charging station to be recharged to upper SOC limit by the rated grid power.

- Ferry at nightlay: When the ferry is at nighlay, zero power is commanded to the charging station's battery. The local grid is slowly recharging the ferry's battery to upper SOC limit and is also providing the requested hotel load supply.

- Ferry docking: When the ferry is connecting / disconnecting to the charging station, zero power is commanded.

- Ferry charging: When the ferry is charging, the rated grid power together with the commanded power from the charging station are transferred to the ferry. The commanded power is pre-determined and constant during the charging period. If the ferry's battery is recharged to upper SOC limit, the controller sets the local grid to supply the hotel load demand on the ferry.

The commanded grid power and ESS power are sent to a cost calculation block where the total power is multiplied with the given electricity price. The instantaneous cost is then integrated during the simulation period to find the total accumulated cost of electricity. Note that the block is only calculating the new energy into the system, meaning that already stored energy in the ESSs are not a part of the calculation. This calculation block is given in Figure C.1 in Appendix C.
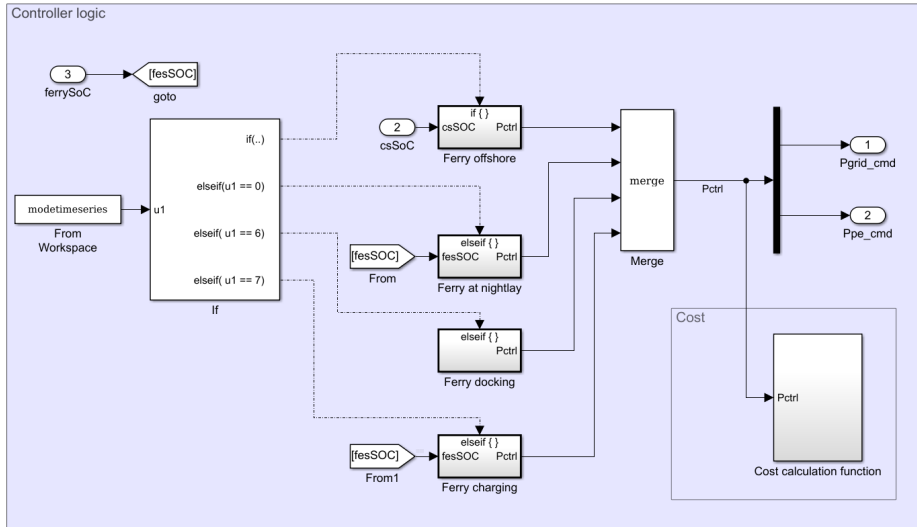
Figure 2.32: The charging station's controller modelled in Simulink

The charging station's ESS is based on the model discussed in Section 2.5.4. The input to the block is the commanded power to or from the ESS, and the output is the actual power transferred to the ferry.

The block also consist of a protection system, given in Figure C.2 in Appendix C, preventing the battery to be charged or discharged outside its rated power and SoC limits. The power out from the protection block is then divided by the terminal voltage, given by a look-up table which outputs the voltage based on the battery's SoC. The obtained current is then going through a gain representing the efficiency factor in the ESS and an integral to calculate the battery's new SoC.
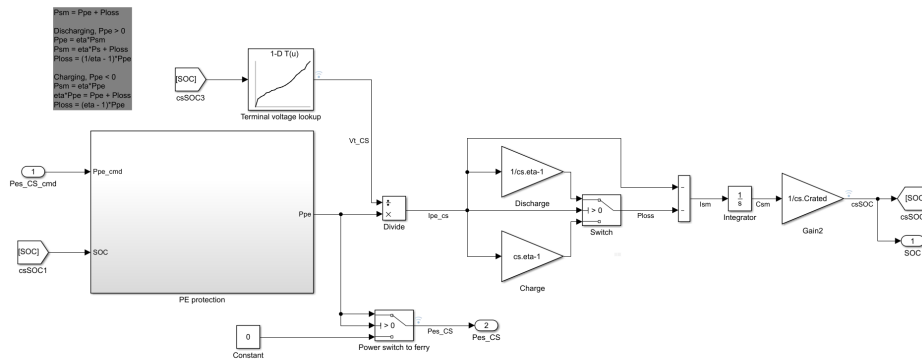
Figure 2.33: The charging station's ESS modelled in Simulink

The Ferry

The ferry block, given in Figure 2.34, consists of a power controller, a load controller, a load module and an energy storage module. The input to the block is the total power coming from the local grid and the charging station and the output is the SoC signal going to the charging station. The load module consists of the ferry load module, given in Figure C.3, and the weather impact module, given in Figure C.4 in Appendix C.
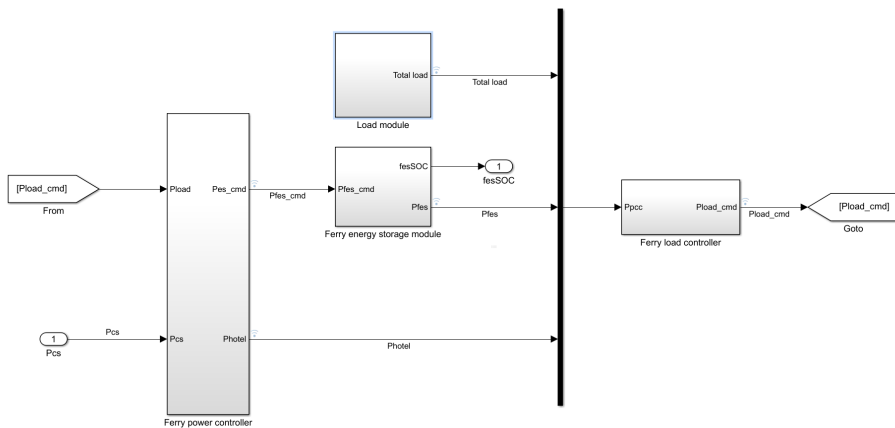
Figure 2.34: The ferry modelled in Simulink

The total load, including propulsion, wind and hotel load, together with the power from the ferry's battery and the power supplying the hotel load when connected to the charging station are connected on a common bus going to the ferry's load controller. The load controller, given in Figure 2.35, acts like a PI - regulator and will always try to control the power from the ESS to meet the load demand.

The load controller brings a more realistic dynamic into the system, resulting in the power balance between the delivered power and the load demand not necessary being always zero. This is caused by the delay introduced in the controller, making the system not able to supply the requested power at instant time.
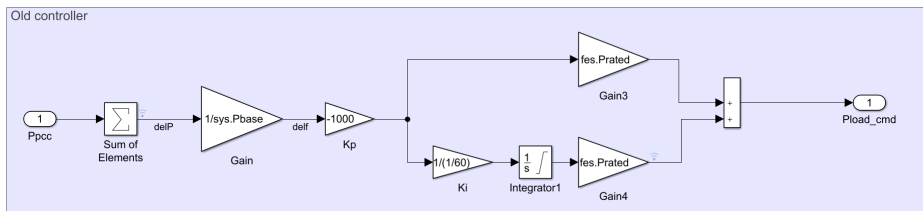
Figure 2.35: The ferry's load controller modelled in Simulink

The controller works fairly well and have a fast response, as seen in the simulation in Figure 2.36. The biggest error of 300 W occurs when the ferry is going from nightlay and directly to acceleration mode. The controller corrects this error in 8 seconds, thus, going from zero propulsion power to 1050 kW is the taking the system 8 seconds.
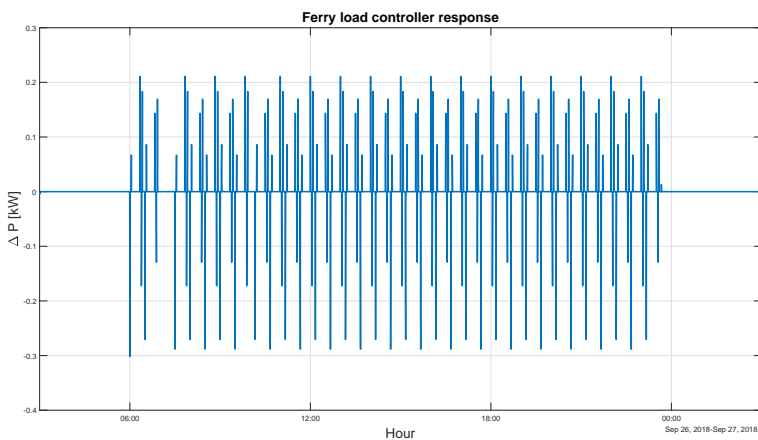
Figure 2.36: ΔP between the load demand and the power delivered

A simpler modelling of the load controller could be to disregard the PI - regulator and instead use a rate of change limiter. The rate limiter could be tuned to achieve equal or better response time and the controller output would be linear.

The ferry's power controller is controlling the power to and from the ferry's ESS. It has two inputs: the commanded power from the load controller and the total power coming from the harbour when charging. The outputs are the commanded power to

the ESS and the delivered power to the hotel load when the ferry is charging.

When the ferry is in transit, the ferry's ESS is delivering all the power necessary to meet the load demand. When the ferry is connected to the charging station, the power from the local grid and the charging station are recharging the ferry's battery and supplying the necessary power to the hotel load. The ferry's ESS is modelled identical to the ESS in the charging station.
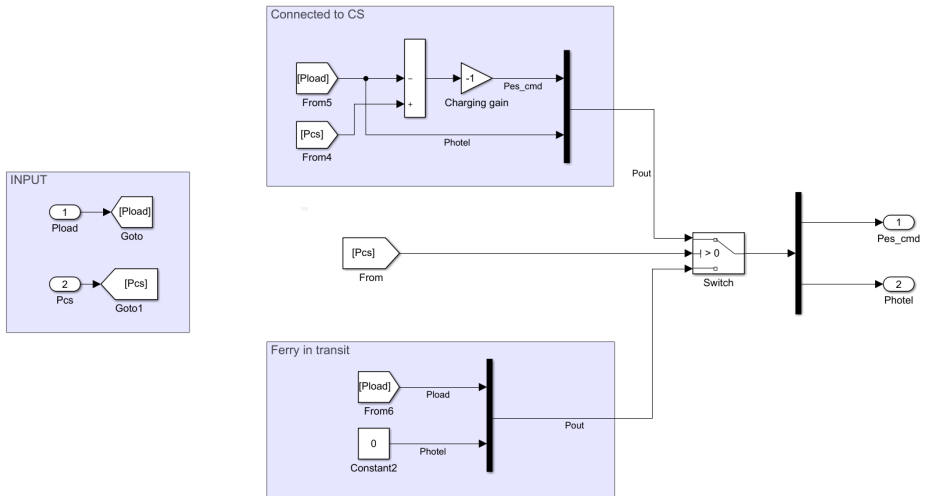
Figure 2.37: The ferry's controller modelled in Simulink

2.7   Model Predictive Control

As the charging strategy presented in Section 3.2.2 is using the principle on model predictive control (MPC) for optimal charging, a brief overview on MPC is given in this section. The theory is based on the formulations given in [49] by D.Q. Mayne et al. and on [50] by B. Foss and T. A. Heirung handed out in the course TTK4135 - Optimization and Control spring 2017.

As formulated by D.Q. Mayne in [49], MPC is a form of control in which the current control action is obtained by solving on-line, at each sampling instant, a finite horizon open-loop optimal control problem, using the current (estimated) state of the plant as the initial state; the optimization yields an optimal control sequence and the first control in this sequence is applied to the plant.

An output feedback MPC procedure is given in Listing 2.1. The algorithm relies on a state estimate which uses available output measurements and is based on Algorithm 3 in [50].

Listing 2.1: Output feedback MPC procedure

```
1  for  t  =  0 ,1 ,2 ,.... do
2          Compute  an  estimate  of  the  current  state  x(t)_hat
                  based  on  the  measured  data  up  until  time  t.
3          Solve  a  dynamic  optimization  problem  on  the
                  prediction  horizon  from  t  to  t  +  N  with  x(t)
                  _hat  as  the  initial  condition.
4          Apply  the  first  control  move  u_t  from  the  solution
                  above.
5  end  for
```

A reference tracking MPC structure with a quadratic objective function and linear constraints is given below. The structure is a modification of Equation 4.4 in [50] and omits the rate of change constraints and the linear penalty function.

$$\min_{z \in \mathcal{R}^n} f(z) = \sum_{t=0}^{N-1} \frac{1}{2}(\hat{\gamma}_t - \gamma^{ref})^T Q(\hat{\gamma}_t - \gamma^{ref}) + d_{\hat{\gamma}}^T \hat{\gamma}_t + \frac{1}{2}u_t^T R u_t + d_u^T u_t + \frac{1}{2}\epsilon^T S \epsilon \quad (2.17\text{a})$$

subject to

$$\hat{x}_{t+1} = A_t \hat{x}_t + B_t u_t \qquad (2.17\text{b})$$

$$\hat{x}_0, u_{-1} = \text{given} \qquad (2.17\text{c})$$

$$\hat{\gamma}_t = H\hat{x}_t \qquad (2.17\text{d})$$

$$\hat{\gamma}^{low} - \epsilon \le \hat{\gamma}_t \le \hat{\gamma}^{high} + \epsilon \qquad (2.17\text{e})$$

$$u^{low} \le u_t \le u^{high} \qquad (2.17\text{f})$$

where

$$Q \in \mathcal{R}^{n_{\hat{\gamma}}} \ge 0 \qquad (2.17\text{g})$$

$$R \in \mathcal{R}^{n_u} \ge 0 \qquad (2.17\text{h})$$

$$\epsilon \in \mathcal{R}^{n_{\hat{\gamma}}} \ge 0 \qquad (2.17\text{i})$$

$$S \in diag\{s_1, ..., s_{n_{\hat{\gamma}}}\}, \quad s_i \ge 0, \quad i = \{1, ..., n_{\hat{\gamma}}\} \qquad (2.17\text{j})$$

The matrices Q, R, S and vectors $d_{\hat{\gamma}}, d_u$ are time invariant and the slack variable ϵ is added to soften the constraints.

The goal in this MPC structure is to track an estimate of the controlled variable, $\hat{\gamma}_t$, which depends linearly on the states, i.e., $\hat{\gamma}_t = H\hat{x}_t$. For a more detailed discussion on the structure and the feasibility of this optimization problem, the paper by Foss and Heirung should be studied.

Chapter 3

Charging Strategies

This chapter will present potential solutions for smarter charging of battery ferries. First, the goals and purpose for smarter charging will be discussed and the objectives presented. The strategies will be divided into two categories: Charging current and energy transfer. The strategies regarding charging current are based on published research in the field of lithium-ion batteries and two different charging methods will be discussed here. Strategies regarding energy transfer are mainly based on an operational view from Siemens and discussions with the supervisors.

3.1   Goals for Smarter Charging

Technical, operational, environmental and economical goals can be included when designing smarter charging strategies for the battery ferry. Different stakeholders may have different objectives regarding their interest, which may conflict with each other.

The technical objectives concerns the battery and power electronic characteristics. Key technical objectives to consider are to minimize the energy losses in transmission, avoid battery temperature increase and battery degradation. A common parameter in all the objectives is the charging and discharging current. As described in Section 2.4.3, a high current will contribute to higher battery temperature and increase the energy losses due to the internal resistance.

The operational objectives concerns the ferry's ability to have sufficient energy capacity to operate the ferry route with minimal delay. Maximize the energy transfer to the ferry when docked and designing battery packs with adequate capacity are key operational objectives to consider. As described in Section 2.4.3, the battery depth of discharge and state of charge have influence on the battery lifetime. Hence, an objective could be to operate the battery state of charge within operational limits.

The economical objectives are a product of both technical- and operational characteristics. To prolong the battery life by optimize the charging current will reduce the system's maintenance costs, while maximizing the energy transfer will increase the operational costs. Taking the electricity prices and weather forecast into account when deciding the energy transfer can provide operational cost savings.

As seen, the different objectives are not independent of each other and trade-offs must be taken when designing smarter charging methods.

3.2   Charging Current Strategies

In this section, two charging current strategies are presented. The first strategy is the constant current - constant voltage method, which is the most common strategy used today. The second strategy considers a model predictive controller and is presented as a pre-study for further work in a master thesis.

There are several techniques to charge a battery, and with the use of better models, more sensors and data processing, the charging is becoming even more advanced. The first charger used in conventional consumer products was the constant current trickle charger. This charger provides a very low constant current rate to the battery and relies on the user to stop the charge when the battery has returned to full capacity. The charger is very economical and simple to design but do nothing to optimize the performance of the battery [51]. A more enhanced version of the constant current charger is the multi-step constant current charger. Here, the current amplitude can be adjusted to a higher value initially and then be lowered towards the end for not to accelerate the battery ageing processes.

Another technique developed is the constant voltage method, which keeps the battery charging voltage constant during the charging process. The charging current is large at the beginning due to the high differential voltage between the terminal voltage

and the internal voltage and decreases towards the end of the process when the internal voltage increases. This follows from Equation (2.6) in Section 2.4.2. The advantage of this method is that the charger is relative simple, and the current will be adjusted automatically to avoid battery ageing phenomena. The disadvantage is the high current at the beginning, which can lead to a high temperature increase and consequently be damageable for the battery [45].

3.2.1 Constant Current - Constant Voltage Strategy

Since the methods mentioned above have some undesired effects of poor performance and potentially insecure behaviour, a method combining both constant current and constant voltage has been developed to improve the charging performance and solving the problems with the two charging methods. This charging strategy is further described below.

The most used charging strategy today is the constant current - constant voltage (CC-CV) strategy. Here, a constant current is applied until the battery voltage reaches a predetermined value, at which the charging voltage is held constant and the current is reduced. The charging stops when the current reaches a minimum threshold value. This method ensures fast charging with constant current when the battery can receive higher current amplitude, and also limits the temperature increase and ageing phenomena in the constant voltage period[51].

However, the constant current - constant voltage charging strategy is very conservative. As stated in [52], the charging profiles are determined by some predefined current and voltage limits irrespective the of battery's *in situ* physical and chemical characteristics. One charging strategy trying the emphasise the internal battery characteristics is presented in the next section.

3.2.2 A Model Predictive Controller Strategy

Model Predictive Control (MPC), elaborated in Section 2.7, can be used for optimal charging of lithium-ion batteries. This is a relatively new approach for battery charging control and has gained more attention in the last years because of its benefits in estimating the battery's SoC and SoH.

In [7] by C. Zou el al. a new charging algorithm, using MPC, for a battery to balance

the competing objectives of battery lifetime and charging time is proposed. The strategy uses a reduced order battery model where the original mathematical representation of the battery, containing coupled electrical, electrochemical, thermal and ageing dynamics, is simplified in a two-step process:

First, time-scale separation techniques are used to decouple the dynamics. This can be done since the electrical dynamics are much faster than the electrochemical-thermal dynamics, which is again significantly faster than the degradation dynamics. Second, the original partial differential equations (PDE) describing the model are reduced to ordinary differential equations (ODE). A further elaboration on this is given in the paper.

A brief presentation of the battery modelling and the outline leading to the overall problem formulation is given in Appendix D. Note that the outline does not cover all parts of the problem formulation and for a more thoroughly description the original paper should be studied.

The overall problem formulation for the MPC charging strategy is given by

$$u_k^* = arg \min_{u_k, s} \sum_{i=0}^{N-1} ||\widehat{y}(i) - y^r(k+i)||_Q^2 + ||s||_\Gamma^2 + ||\widehat{y}(N) - y^r(k+N)||_{P_k}^2 \qquad (3.1a)$$

$$\text{subject to } \forall i \in \{0, ..., N-1\} \qquad (3.1b)$$

$$\widehat{x}(i+1) = A_k \widehat{x}(i) + B_k u(i) + \widehat{d}_k \qquad (3.1c)$$

$$\widehat{y}(i) = C\widehat{x}(i) \qquad (3.1d)$$

$$\widehat{x}(0) = \widehat{x}_k \qquad (3.1e)$$

$$-I_{max} \leq u(i) \leq 0 \qquad (3.1f)$$

$$M\widehat{x}(i) \leq c_0 + s \qquad (3.1g)$$

$$s \geq 0 \qquad (3.1h)$$

where the decision variable, u_k^* is the optimal sequence of the predicted charging current input to the battery over the prediction horizon. Only the first input, $u^*(0)$, is applied to the system.

The system outputs of interest, $y(i)$, are defined to be

$$y(i) := \begin{bmatrix} SOC(i) & \Delta SOH(i) \end{bmatrix}^T$$

$$\Delta SOH(i) := SOH(i) - SOH(i-1),$$

(3.2)

and hence, the cost function contains two competing objectives: namely maximizing the charge rate whilst simultaneously minimizing the change in SoH. The notation $||\cdot||^2$ is interpreted as the squared weighted 2-norm, i.e., $||x||_Q^2 = x^T Q x$.

The input constraint in Equation (3.1f) is adding a upper value to the charging current and the constraints for the estimated states in Equation (3.1g) are adding an upper limit on the temperature and limits for the lithium-ion concentration in the battery. Because of uncertainty of violating these constraints, they are implemented as soft constraints by introducing the slack variable s. Under this relaxation, the term $s^T \Gamma s$ is added as a penalty function to the cost function.

The proposed control algorithm is illustrated in Figure 3.1. For given references, SOC^r and SOH^r, and state information from the estimator $\widehat{x}_k$, the designed MPC controller calculates the optimal input current, u_k^* at each time step k.
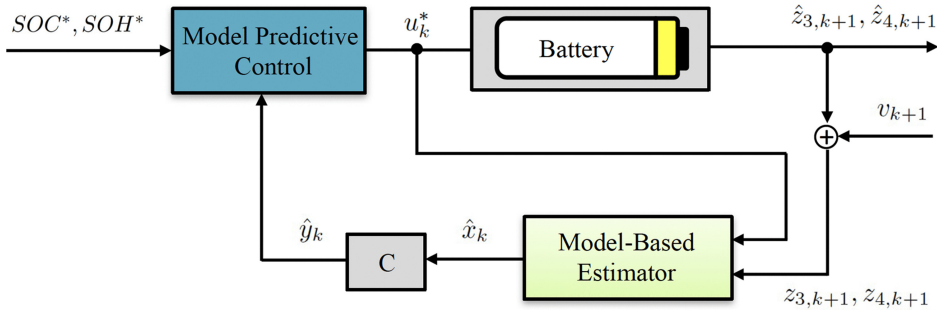

Figure 3.1: Illustration of MPC algorithm for battery charging. Taken from [7]

As described in [52], the charging strategy presented here have two benefits: it is able to reduce the battery's charging time and increase the battery lifetime; and it offers flexibility to manipulate battery degradation or the charge profile as desire.

3.3   Energy Transfer Strategies

By looking at the energy transfer between the charging station, the ferry and the local grid, the charging strategies are changed from a technical perspective to a more operational perspective.

In an operational perspective the controller is controlling the amount of energy transferred between the systems based on both internal and external parameters. Internal parameters can be operational limits in the battery such as SoC and power limits and external parameters can be weather conditions impacting the ferry during transit, available grid power considerations, electricity prices and power losses during transmission among other things.

There exist a lot of research on optimal scheduling for energy transfer to charge electric vehicles and much of this is applicable to use in battery ferries. In [53], Y. He et al. formulates a global scheduling optimization problem, in which the charging powers are optimized to minimize the total cost of electricity of all electric vehicles which perform charging and discharging during the day. By some adjustment, this optimization problem could be used to design an optimal charging strategy for the ferry.

In the next chapter, two different energy transfer strategies for charging the ferry are studied: A strategy considering weather conditions and a strategy considering electricity pricing. The controllers are not based on optimal algorithms for energy transfer, but rather trial and error to find the best way to charge the ferry when considering external parameters.

Chapter 4

Energy Transfer Optimization

In this chapter, two strategies for more optimal energy transfer between the charging station and the ferry are studied. The first strategy is considering the weather conditions for better planning of energy transfer. The second strategy is taking the electricity price variations into account when planning the energy transfer.

The two strategies are independent of each other, meaning that the weather conditions will not conflict when deciding the energy transfer with regards to the electricity pricing. This is a simplification compared to a realistic system, but is chosen for better see the potential, benefits and disadvantages of the strategies.

A reference system is presented first to be further used in comparison with the other study cases. An important parameter when comparing the study cases is the power from the charging station, P_{CS}, which directly influences the SoC in both the charging station and the ferry, the total energy used and the total accumulated cost of electricity during the simulation period.

4.1 Reference System

The reference system is following the operational profile given in Section 2.5.5 and is not taking the weather conditions and electricity pricing into account. As seen in Figure 4.1, the power delivered to the ferry when charging is always the same, giving the SoC profiles for the ferry's and charging station's battery in Figures 2.23 and 2.24, respectively.
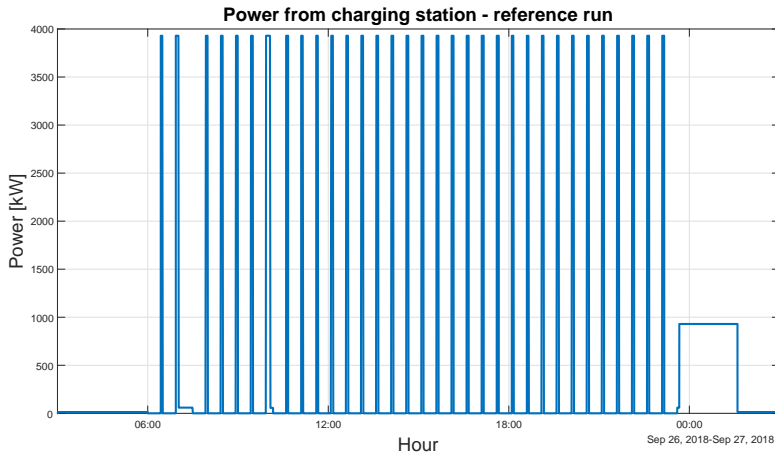
Figure 4.1: Power from charging station to ferry, P_{CS}, under normal run

The key results from the simulation of the reference system are given in Table 4.1. The battery in the charging station has its highest DoD (32 %) at 10:00, when the ferry's battery is recharged from 54% and up to 65%. In a normal charging cycle with a charging time of 4 minutes, the battery in the charging station is cycled with a DoD of 15 %, which increases the ferry's battery SoC by 5.1%.

Because the energy balance between the consumed energy and the delivered energy to the ferry is negative, the ferry's battery SoC is decreasing throughout the simulation period. After the last crossing, the SoC has decreased down to 29%, resulting in a DoD of 36% from the upper SoC limit. Remark that this is under ideal weather conditions with a constant wind speed of 2.5 m/s and a predicted operation of the ferry.

The average charging station DoD at each harbour is used as an indicator for the overall utilization of the battery. In the reference system, the average at harbour 1 and

harbour 2 are respectively 16% and 15%, meaning we have a higher overall utilization of the battery in the charging station at harbour 1. Looking at the highest DoD cycle, the battery in the charging station at harbour 1 is cycled 11% deeper than the battery in the other charging station.

Table 4.1: Key results after normal run

Result	Value	Unit
Total energy consumed	10330	kWh
Total cost of electricity	4834	NOK
Lowest ferry SoC	29	%
Ferry DoD	36	%
Highest CS DoD (Harbour 1)	33	%
Highest CS DoD (Harbour 2)	22	%
Average CS DoD (Harbour 1)	16	%
Average CS DoD (Harbour 2)	15	%

In a real operating ferry system, the charging power is determined by the available grid and charging station power and the limitations in the power transmission. The overall objective for the charging strategy used today is to maximize the energy transferred to the ferry. Hence, the charging power can be seen as relatively constant, making the reference system presented in this section more equal a real operating system.

4.2   Study Case: Weather Conditions

In this study case, the ferry's load profile is influenced by the varying weather conditions. The weather characteristic presented in Section 2.5.6 is used to model the weather conditions during the simulation period. As discussed, the factor contributing to the load variation is the wind effect on the ferry.

4.2.1   Objective

Since it is assumed that the wind speed and wind direction are known before the charging process begin, the controller in the charging station can decide how much extra or less energy that is necessary to transfer during the charging period.

Two objectives are chosen for this study case: The first objective is to control the amount of energy that is transferred in each charging cycle to obtain the same SoC, within ± 1%, as the reference system's SoC at the end of the day. Hence, to have a SoC in the range 28% to 30% at the time the ferry is going back to nightlay-mode.

The second objective is to satisfy the upper and lower SoC limit in the charging station's ESS and operate within the power transmission limits.

4.2.2   Operational Profile

The profile for the wind load is given in Figure 4.2. This profile is calculated by using Equation (2.14) and the values for the wind speed given in Figure 2.26. As seen, the wind load is positive and negative, illustrating the ferry experiencing both headwind and tailwind. Usually, the ferry experiences headwind in one crossing and tailwind in the next, but when the wind direction suddenly changes, the ferry can experience headwind or tailwind in both crossings.

In the model, the wind load is added to the normal operational profile, giving the new load profile for the ferry, as shown in Figure 4.3. Since the wind speed is higher in the morning and before noon, the impact on the ferry load is bigger in this period.

While the ferry load is constant in each mode of operation, the wind load can vary. This is easiest seen in the operational profile by the positive and negative slopes when the ferry is in transit mode. The energy used during the simulation period is calculated to 10399 kWh, which is 69 kWh more than the energy used in the normal operational
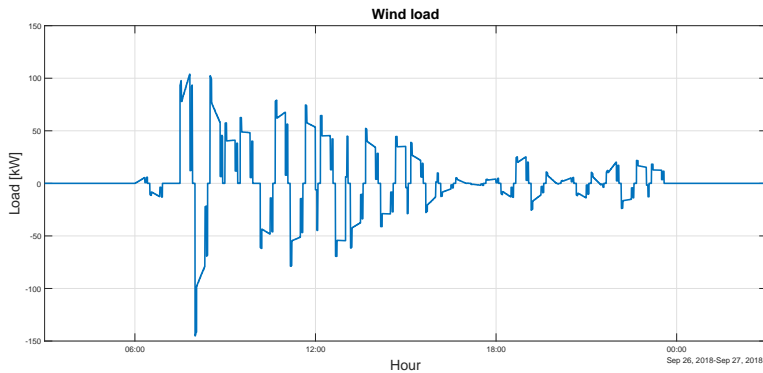
Figure 4.2: Load impact on ferry caused by wind

profile. Hence, the ferry is affected more by headwind than tailwind.

To compensate for the additional load demand, the energy delivered to the ferry should increase with approximately the same amount. The profile for the power transferred to the ferry is given in Figure 4.4. As seen, the power is not the same in each charging cycle, varying from 3537 kW and up to maximum allowable power of 4323 kW. These values are ± 10% of the normal charging power used in the reference system.

The controller is deciding the power transfer based on the upcoming weather conditions for the crossing, meaning that when a tailwind with speed above 5.0 m/s is predicted, the controller is reducing the power transferred. On the contrary, when the predicted weather shows headwind and a wind speed above 5.0 m/s, the controller is increasing the power transferred. The controller strives to satisfy this charging strategy but it is not strictly followed because the controller also need to take the ferry's SoC into account.
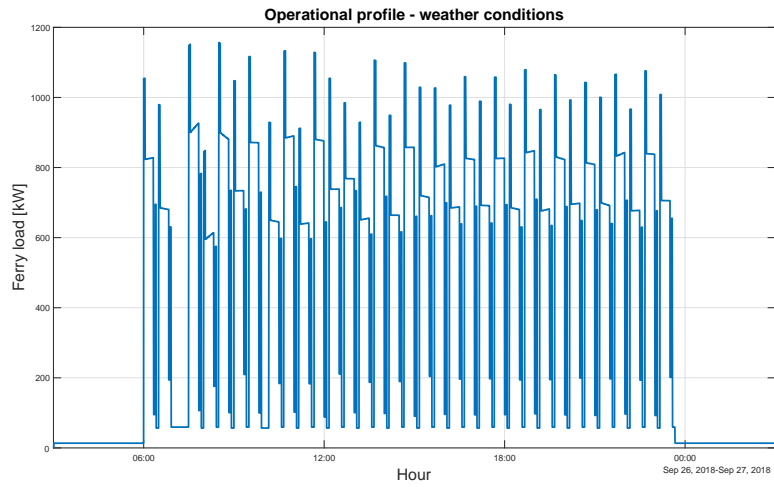
(a) Operational profile over 1 day
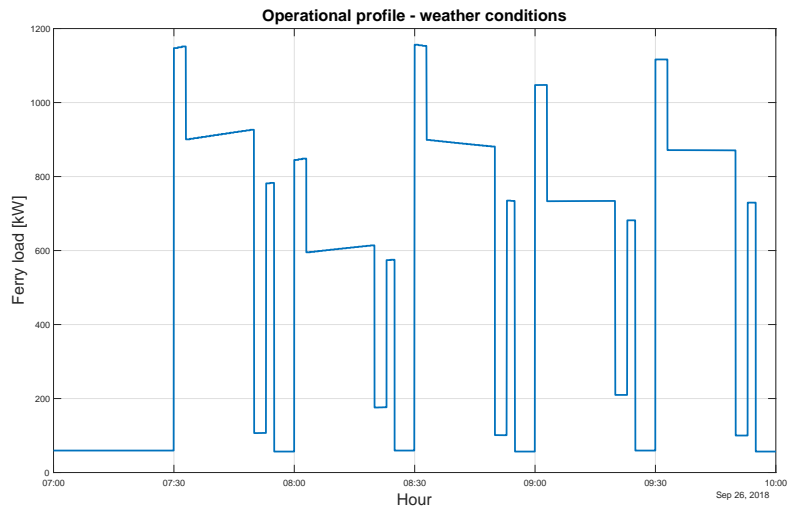
(b) Operational profile of ferry from 07:00 to 10:00

Figure 4.3: Operational profile under weather conditions
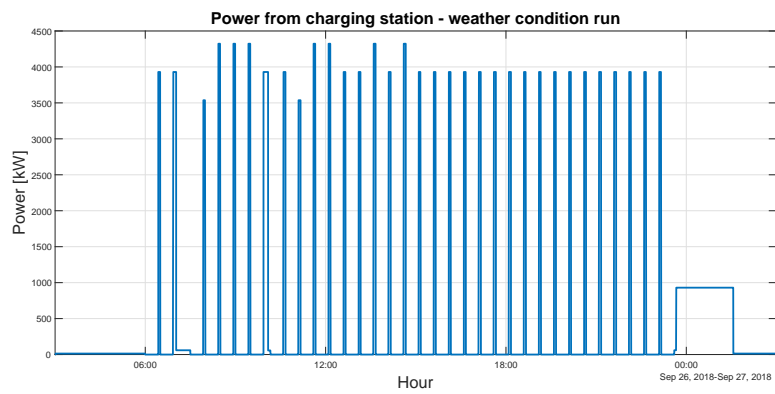
Figure 4.4: Power from charging station to ferry under weather conditions

4.2.3   Results

As seen in the SoC profile for the ferry's battery, given in Figure 4.5, the SoC at the end of the day is 30%. Comparing this to the reference system, the SoC is increased by 1%. The SoC profile for the battery in the charging station, given in Figure 4.6, shows that the battery is always operated within the limits. Hence, the two objectives for the study case are fulfilled.

The other blue curve in the SoC profile for the ferry's battery is the SoC profile for the reference system. Comparing the simulations when the wind speed is at its highest during the morning and before noon, the profiles are following each other fairly well. Towards the afternoon, the SoC profile under weather conditions is decreasing more slowly than the reference system. This is caused by the increase in energy transfer at 13:40 and 14:40 at harbour 2.
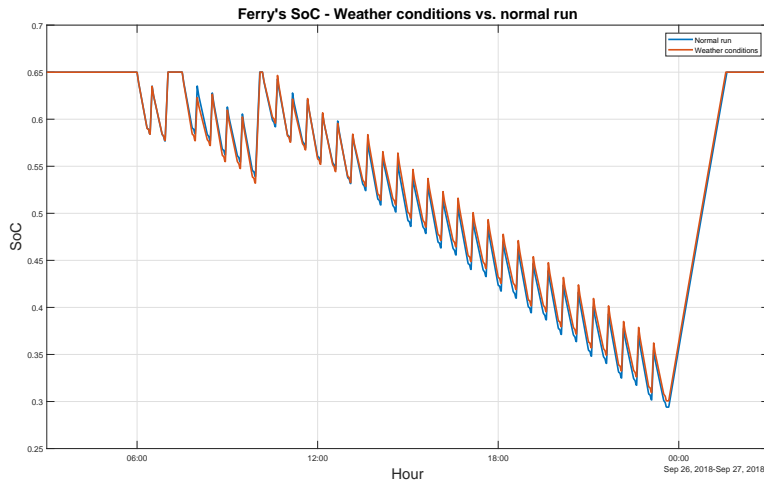
Figure 4.5: Ferry's SOC under weather conditions

Assumed the grid power remains constant, less energy transferred to the ferry implies lower DoD for the battery in the charging station and more energy transferred implies higher DoD. Comparing the charging station's SoC profile under weather conditions in Figure 4.6 to the reference system in Figure 2.24, the most important difference is that the highest DoD at harbour 1 is increased with 3%. This means higher utilization

of the battery, which in a real system would result in a negative effect on the battery's SoH.
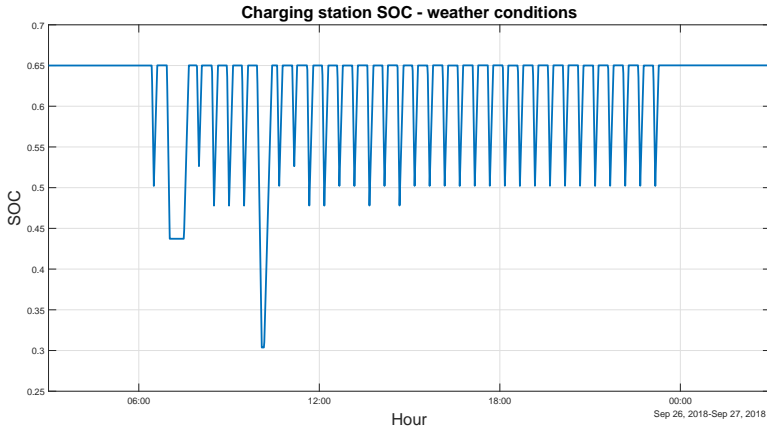
Figure 4.6: Charging station SOC under weather conditions

The key results for the study case are listed in Table 4.2. Comparing the results to the reference system, the average CS DoD at harbour 2 is increased with 1%. This is natural, since more energy is transferred to the ferry because of the increase in energy consumption.

Table 4.2: Key results after run considering weather conditions

Result	Value	Unit
Total energy consumed	10399	kWh
Lowest ferry SoC	30	%
Ferry DoD	35	%
Highest CS DoD (Harbour 1)	35	%
Highest CS DoD (Harbour 2)	21	%
Average CS DoD (Harbour 1)	16	%
Average CS DoD (Harbour 2)	16	%

4.2.4   Further Considerations

Since the battery capacity in the ferry is very large, the wind effect is not impacting the system as much as predicted. This is seen by calculating the contribution from the additional energy consumed by the ferry to the effective storage. With an effective storage of approximately 2176.2 kWh in the ferry, the additional 69 kWh consumed is only 3.1% of the capacity.

If the ferry is operated in a place with statistically more wind from one direction than the other, some factors on the operation of the charging stations must be considered. Using the charging strategy above, one charging station would be more utilized than the other, and hence, the battery degradation over time in the two charging stations would not be equal. A technical and an operational study should then be performed to analyse the difference in letting the SoH in each charging station not be equal.

Some reflections around the weather model used should also be mentioned. The model is only based on qualitative guessing of the impact on the ferry load by the wind speed. Consequently, converting this charging strategy to a real system could yield unsatisfying results.

4.3 Study Case: Electricity Pricing

In this study case, the controller is considering the current and forthcoming electricity price when deciding the amount of energy transferred to the ferry. Because of high variations in electricity price during the day, the potential of scheduling the energy transfer to periods with lower electricity cost for savings is studied.

The adjusted electricity price dynamic, given in Figure 2.28, is used by the controller as a decision basis, and it is assumed that the controller knows the forthcoming prices before the energy transfer is calculated.

4.3.1 Objectives

The objectives in this study case will be to reduce the overall electricity cost compared to the reference system and to operate the system within the operational limits.

4.3.2 Operational Profile

The operational profile for the ferry is identical to the reference system given in Figure 2.22 and no external factors are impacting on the ferry load under operation. As seen by the price dynamic in Figure 2.28, the price of electricity is at its highest in the morning (around 08:00) and in the evening (around 17:00), and consequently there is beneficial to transfer less energy to the ferry in these time regions.

As seen in Figure 4.7, the controller in the charging station is adjusting the power output between three different values. The normal charging power, used in most of the charging cycles, is 3930 kW. When the electricity price is high, the controller reduces the power output down to 1965 kW, which is a decrease of 50% from the normal power output. When the electricity price is low or when more energy is necessary to transfer to satisfy the battery SoC in the ferry, the controller is increasing the power output to 4323 kW, which is the maximum allowable power output and an increase of 10% from normal power output.
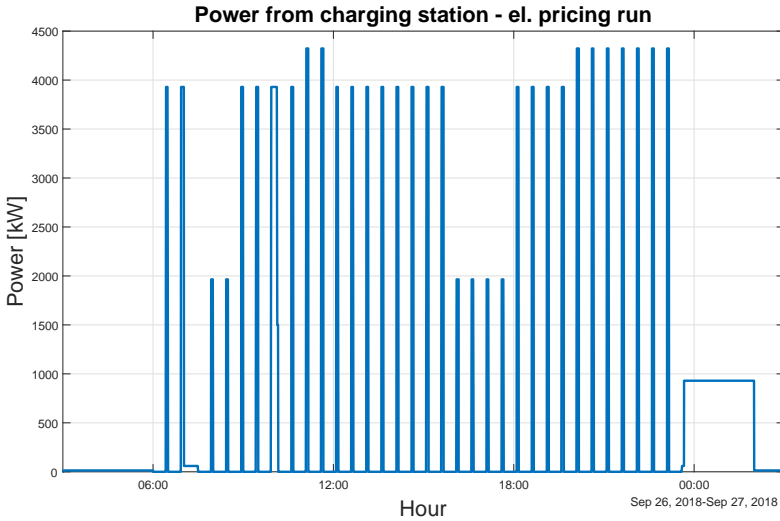
Figure 4.7: Power from charging station to ferry with respect to electricity pricing

The instantaneous cost of electricity is given in Figure 4.8. As seen, the bars in the figure are following the electricity price dynamic and the amplitude of the bars are illustrating the cost of the system at a given time during simulation. To reduce the overall cost of electricity, it is necessary to decrease the areal under the bars with highest amplitude. In a system context, since the grid power is constant, this means to limit the recharging time of the battery in the charging station by transferring less energy to the ferry.

4.3.3   Results

The resulting SoC profiles for the ferry and the charging station are given in Figures 4.9 and 4.10, respectively. Comparing these profiles against the reference system, there are some important differences.

When the controller is reducing the power output, only 131 kWh is transferred to the ferry in one charging cycle, resulting in a negative energy balance of 179.2 kWh in leg 1 and 144.6 kWh in leg 2. This causes the SoC in the ferry's battery to rapid decrease, as seen around 08:00 and 16:40 in Figure 4.9. To avoid operating the ferry's battery
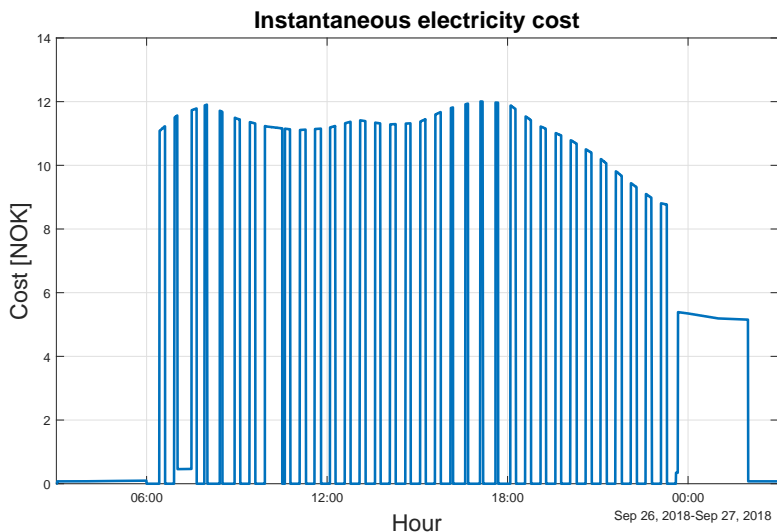
Figure 4.8: Instantaneous electricity cost

outside the SoC limits, maximum power is transferred during the evening when also the price of electricity is low.

At the end of the day, the SoC in the ferry's battery is 22%, which is a reduction of 7% compared to the reference system. This is caused by less energy being overall transferred to the ferry. In an operational view, having only 2% clearing from the lower SoC limit will not be satisfying for the operators and in a technical view, cycling the battery with a DoD of 43% will have more negative effect on the battery lifetime compared with the reference system.

The battery in the charging station at harbour 1 is deep cycled down to the lower SoC limit once during the simulation period. This occurs when the ferry has a longer pause at 10:00 and the battery in the ferry is recharged to 64%. The average DoD in the batteries at harbour 1 and 2 are respectively 15% and 14%, meaning the utilization is lower compared to the reference system.
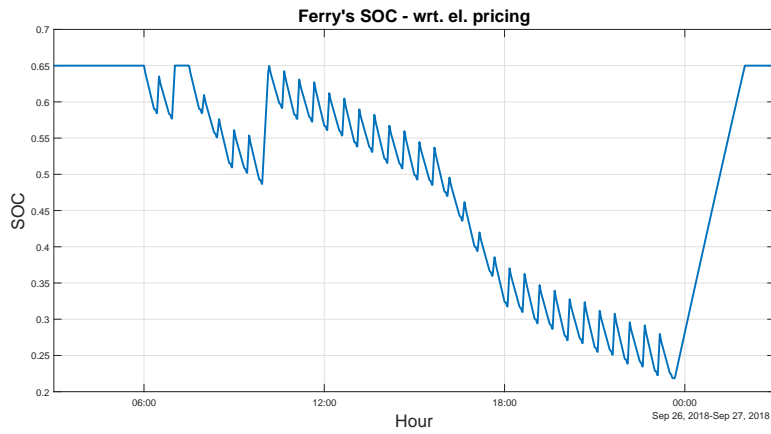
Figure 4.9: Ferry's SOC with respect to electricity pricing
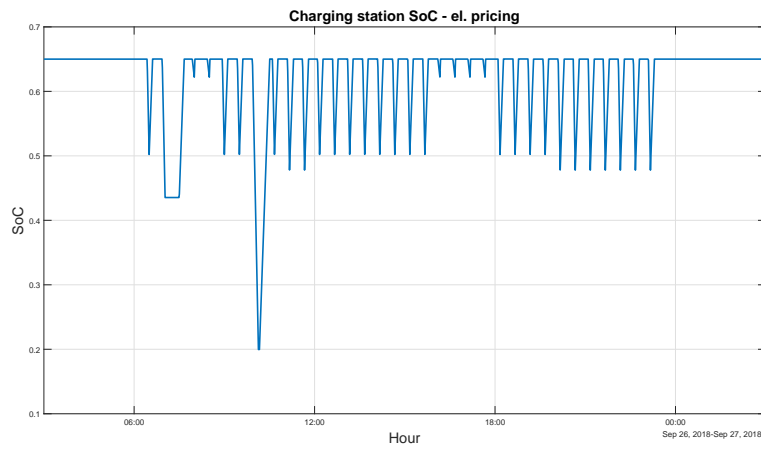
Figure 4.10: Charging station SOC with respect to electricity pricing

The accumulated cost of electricity for this system compared to the reference system is given in Figure 4.11. The blue curve is representing the system taking the electricity price into account and the red curve is representing the reference system. As seen, the difference between the systems becomes bigger towards the evening, when the electricity price is high and the controller is reducing the power transferred to the ferry. Overall, the total cost of electricity in the system accumulated to 4779 NOK, which is a reduction of 1.1% from the reference system.

An important observation from the figure is the difference in cost between the systems in the morning which becomes negligible after the pause at 10:00. Since less energy is transferred to the ferry under the high electricity price period in the morning, more energy is transferred during the pause at 10:00, making the overall energy transferred almost equal the reference system. A better charging strategy would here be to charge the ferry's battery in the same manner as the reference system during the morning and thus have more capacity to use for savings during the evening.
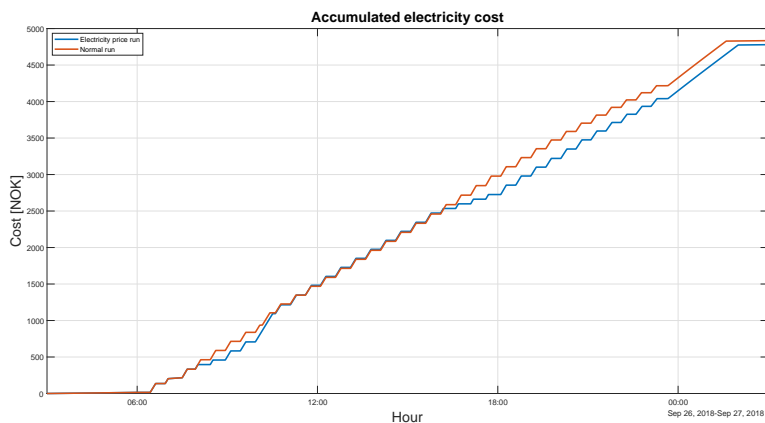
Figure 4.11: Accumulated electricity cost

The objectives for the study case are fulfilled with a small remark on the battery in harbour 1 which is cycled down to lower SoC limit at one instance. The key results are listed in Table 4.2.

Table 4.3: Key results after run considering electricity pricing

Result	Value	Unit
Total energy consumed	10330	kWh
Total cost of electricity	4779	NOK
Savings	1.14	%
Lowest ferry SoC	22	%
Ferry DoD	43	%
Highest CS DoD (Harbour 1)	45	%
Highest CS DoD (Harbour 2)	35	%
Average CS DoD (Harbour 1)	15	%
Average CS DoD (Harbour 2)	14	%

4.3.4   Further Considerations

Since the battery utilization in the ferry is higher when taking the electricity price into account, the reduction in cost should be considered up to the long term battery degradation. If the acceleration in battery degradation is larger than the savings, the charging strategy proposed here would not be profitable.

It could be beneficial to change the time of the pauses to periods with lower electricity prices. As an example, an operational profile with just one large pause, lasting 30 minutes, at 10:30 is simulated. The SoC profile for the ferry's battery is given in Figure 4.12 and as seen, the SoC is going under the lower SoC limit and ends on 19%. However, the cost is accumulated to 4758 NOK, which is a reduction of 1.6% from the reference system.

Allowing both changes to the ferry schedule and going outside the operational limits adds new degrees of freedom to the problem. Further work with sensitivity analyses with regards to cost savings could exploit new ways for better charging the ferry.
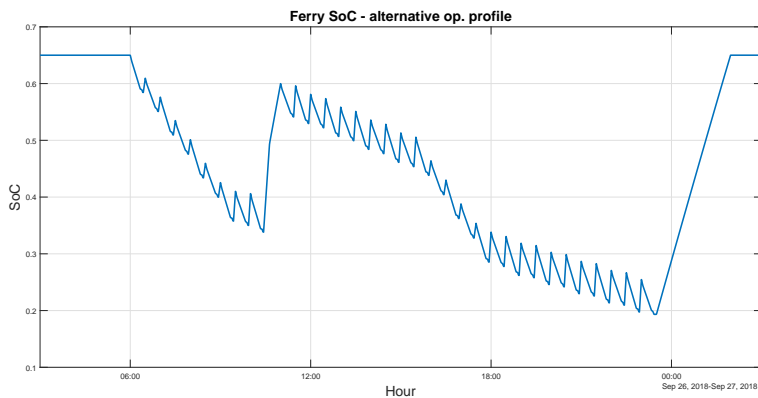
Figure 4.12: Ferry SoC with alternative operational profile

In this study case, only the battery in the ferry is considered when controlling the power transfer. Rejecting the battery in the charging station to fully recharge under periods with high electricity price and varying the power transfer to the battery in a same way as the battery in the ferry, could further reduce the overall costs.

A more complex controller with dynamic output, which allows the power transfer to be more varied, could be beneficial for the performance of the system. This controller could take use of a mathematical approach for finding the optimal amount of energy to be transferred.

Chapter 5

Conclusion & Future Work

In the first part of the report, an overlook of the history towards the modern battery ferry is given with a discussion on the different shipboard power systems and two examples of operating ferries in the Norwegian transportation network. An example on a ferry control system is then proposed, with a brief presentation on the control objectives for the different components in the system.

A discussion on different battery types and technologies, with an elaboration on the lithium-ion battery ageing phenomena is then given. Furthermore, the system modelling and the Simulink implementation for use in the simulations are presented.

In the second part, strategies for charging the ferry are discussed. The constant current - constant voltage strategy and the more complex model predictive controller strategy are presented with a discussion also on energy transfer strategies.

The chapter also presents some of the key parameters that are necessary for planning the charging of a ferry more efficient. The parameters are summarized in the following list:

- The charging current: influences the energy losses, battery temperature and battery degradation.

- The battery DoD: influences the ferry operation, battery utilization and battery degradation.

- The weather conditions: influences the battery utilization.

- The electricity pricing: influences the operational costs.

- The available grid power: influences the battery utilization.

In the last part, a reference system, a system with varying weather conditions and a system considering electricity pricing are simulated and compared to each other. A energy transfer controller for each of the two last systems are proposed with the purpose of smarter charging the ferry.

In the system with varying weather conditions, the battery at harbour 2 is more utilized compared to the reference system, which is caused by the controller taking the SoC in the ferry's battery into consideration when deciding the energy transfer. In the system considering electricity pricing, the overall utilization of the battery at each harbour is reduced compared to the reference system. However, the ferry's battery is more utilized and operates closer to the operational limits. This is caused by the controller taking economical considerations when deciding the energy transfer. It is seen by changing the time of the pauses, the cost of electricity could be further reduced.

The writer's opinion is that an energy transfer controller could be beneficial for more predictable and effective utilization of the batteries in a ferry system as the one presented here.

The simplified weather model and battery model, together with the relatively constant operational profile, are some of the key factors that deviates this system from a realistic system. Since the study cases also are isolated from each other it is hard to say how a controller in a real system would perform.

As the writer will continue with a MSc project on this topic, a brief discussion on further work and possibilities within smarter charging of battery ferries will be presented in the following.

System modelling

Developing a more scalable model of the system, with incorporation of a suitable current charging strategy for the battery, should be considered for future work. With scalable it is meant a model which is built for easily changing its attributes, i.e., adding more ferry systems, operational profiles or changing the charging station characteristics. A such system could further be used for better sensitivity analyses of future control strategies.

Limitations in equipment with regards to power transmission could be included to improve the model. For better validating the performance of the model, the results should also be compared to actual data from real operating ferries.

Weather and load model

For future work, a more realistic and proven weather model should be considered. Factors such as the vessel's angle towards the wind and waves, the vessel's frictional resistance towards the water working against movement and the actual wind impact on the ferry should be studied.

In this study, an almost constant load model is used for the simulations. In a realistic system, the load would vary throughout the day as the number of cars and passengers on the ferry is not constant. For better load estimation in the controller, the load variation should therefore be taken into account.

Charging controller

Designing a more advanced charging controller should be a focus for future work. By obtaining better models for the weather and load, a more advanced controller could predict the energy used in one crossing and propose an optimal value for the transferred energy. A cost function minimizing the difference between the predicted energy consumption and energy delivered with respect to the electricity price and battery lifetime could be suitable for the charging strategy.

Grid power considerations

A future study on the impact of variable available power from the grid could be performed. In such a case, the ferry could take more power from the grid when this was available for reducing the utilization of the battery in the charging station.

A cloud system, such as Mindsphere from Siemens, illustrated in Creffig:mindsphere, could be used to collect data from the charging stations and the ferry. In addition, if the cloud system started to collect data from the substations, the available power from the grid could be implemented in the controller design.

Figure 5.1: Communication between substation, charging stations and ferry[9].

Some of the potential in smarter charging of battery ferries is given in this report and much more can be considered when looking at the possibilities. With willingness to realize the potential benefits, an even more sustainable ferry system could be within reach.

Appendix A

Weather Model

Table A.1: Weather data from Sandane Airport Weather Station. Data from [6]

Hour	Temperature [°C]	Rainfall [mm]	Wind [m/s]	Wind Direction
03	8.9	0.0	6.1	E-NE
04	9.7	0.0	4.0	E-NE
05	9.4	0.0	3.4	E-NE
06	9.5	0.0	2.5	NE
07	10.4	0.0	3.7	N-NW
08	10.2	0.0	11.2	NW
09	10.8	0.0	8.0	W
10	9.3	0.0	6.4	W-NW
11	10.4	0.0	8.1	W-NW
12	10.2	0.0	6.9	W-SW
13	11.1	0.0	7.0	W-NW
14	11.2	0.0	5.3	W-NW
15	9.2	0.0	5.4	W-SW
16	8.9	0.0	3.3	N-NE
17	10.1	0.0	2.5	N-NE
18	10.1	0.0	2.8	NW
19	9.5	0.0	4.6	W-NW
20	8.5	0.0	2.5	W-NW
21	9.5	0.0	1.6	N-NE
22	8.4	0.0	3.7	N
23	8.8	0.0	3.6	SE
00	8.0	0.0	3.3	N
01	8.0	0.0	2.1	N-NE
02	7.7	0.0	3.2	N-NW
03	7.2	0.0	1.2	W

Appendix B

Matlab Code

Listing B.1: Configuration file

```
1   %% Configuration file
2
3   %% System properties
4   sys.Pbase        = 1200e3;
5   sys.windfactor   = 1/(50-2.5);
6   sys.wind_avg     = 2.5;
7
8   %% Load data
9   profile                  = load_battery_profile();
10  loadtimeseries           = profile.totpwr;
11  quaytimeseries           = profile.leg;
12  modetimeseries           = profile.modenum;
13  chargetimeseries         = profile.chrgpwr;
14  elpricetimeseries        = profile.elprice;
15  windtimeseries           = profile.wind;
16  winddir.time             = profile.wind_dir(:,1);
17  winddir.signals.values   = [profile.wind_dir(:,2),
        profile.wind_dir(:,3)];
18  winddir.signals.dimensions = 2;
```

```
19  chargetimeseries(isnan(chargetimeseries)) = 0;
20
21  %% Power grid data
22  Pgrid_rated = 1500e3; % Assuring sufficient power flow
        from grid
23
24  %% Charging station specifications
25  cs.Prated  = 4140e3;
26  cs.Vrated  = 930; % [V]
27  cs.Crated  = 1200*60; % [Ah]
28  cs.C_0     = 0.65*cs.Crated;
29  cs.SOClower = 0.2;
30  cs.SOCupper = 0.65;
31
32  cs.Ppe_upper = cs.Prated;
33  cs.Ppe_lower = -cs.Prated;
34  cs.eta = 0.97;
35
36  %% Ferry energy storage module specifications
37  fes.Prated    = 4140e3;
38  fes.Vrated    = 930; % [V]
39  fes.Crated    = 2*2600*60; % [Ah*min/h]
40  fes.C_0       = 0.65*fes.Crated;
41  fes.SOClower = 0.15;
42  fes.SOCupper = 0.65;
43
44  fes.Ppe_upper = fes.Prated;
45  fes.Ppe_lower = -fes.Prated;
46  fes.eta = 0.97;
```

Listing B.2: Script for loading operational profile

```matlab
1  %% Function to load battery profile from excel
2  % and wind- and electricity price profiles
3
4  function profile = load_op_profile ()
5      [num, txt] = xlsread ('OperationalProfileWeather.xlsx')
            ;
6      load adj_elprices ;
7      load anda_wind ;
8      load anda_wind_dir ;
9
10     profile . min           = num (: ,1) ;
11     profile . time          = num (: ,2) ;
12     profile . leg (: ,2)     = num (: ,4) ;  profile . leg (: ,1) =
            profile . min ;
13     profile . modenum (: ,2)  = num (: ,6) ;  profile . modenum (: ,1)
            = profile . min ;
14     profile . totpwr (: ,2)   = num (: ,10) *1000;  profile . totpwr
            (: ,1)  = profile . min ;
15     profile . chrgpwr (: ,2)  = num (: ,12) *1000;  profile .
            chrgpwr (: ,1)  = profile . min ;
16
17     %% El . price timeseries
18     adj_elprices = adj_elprices *(1/1000) *(1/1000) *(1/60) ;
            % [NOK / Wmin]
19     t = 0:60:1440;
20     t = t ';
21     tt = 1:1440;
22     adj_elprices = interp1 (t, adj_elprices , tt ) ;
23     profile . elprice (: ,2)  = adj_elprices ;  profile . elprice
            (: ,1) = profile . min ;
24
25     %% Wind timeseries
```

```matlab
26         anda_wind = interp1 (t , anda_wind , tt );
27         profile.wind(: ,2) = anda_wind ; profile.wind(: ,1) =
              profile.min;
28
29         profile.wind_dir(: ,2) = anda_wind_dir(: ,1); profile.
              wind_dir(: ,1) = profile.min;
30         profile.wind_dir(: ,3) = anda_wind_dir(: ,2);
31  end
```

Appendix C

Simulink Diagrams

Cost calculation module
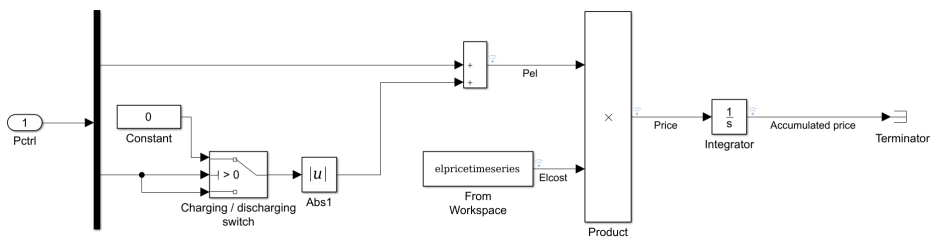

Figure C.1: Cost calculation function modelled in Simulink

## Protection module in the ESS
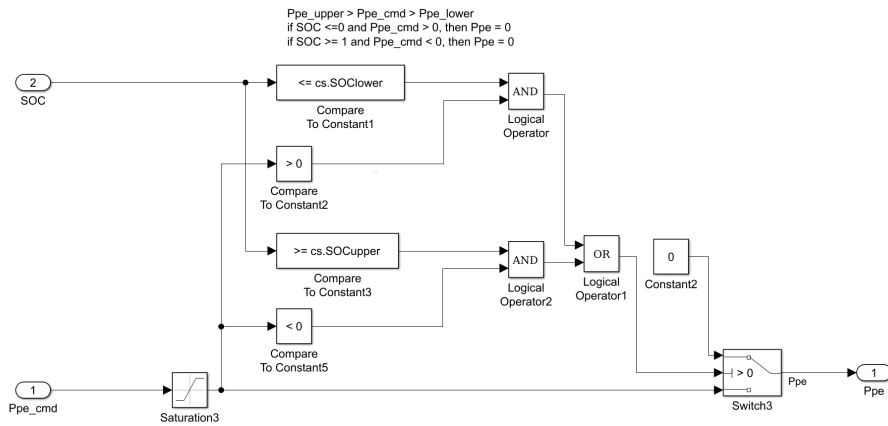
Figure C.2: ESS protection module modelled in Simulink

Ferry load module
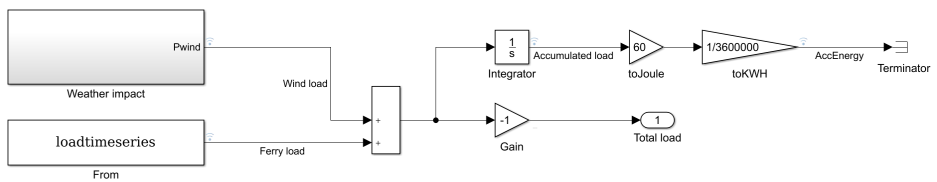
Figure C.3: Ferry's load module modelled in Simulink

Weather impact module
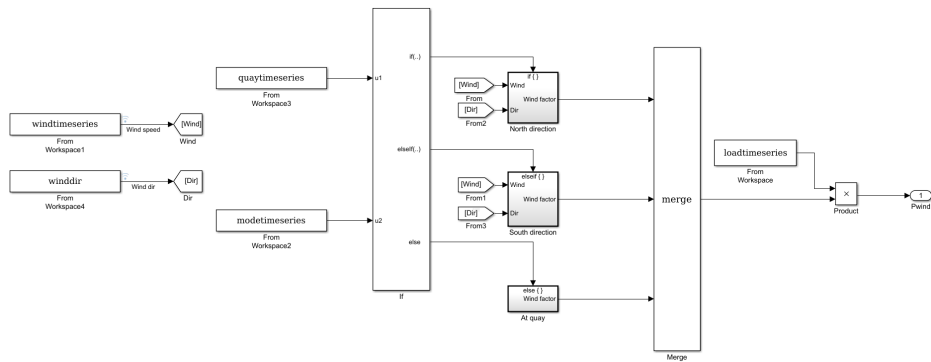
Figure C.4: Weather impact module modelled in Simulink

Appendix D

MPC Problem Formulation

Table D.1: Nomenclature for the MPC charging strategy[7]

Input:	
I	Applied current
Variables:	
C_e	Lithium-ion concentration in the electrolyte
C_s	Bulk lithium-ion concentration in solid particles
C_{ss}	Lithium-ion concentration at the surface of solid particles
q_s	Concentration flux at the surfaceof solid particles
Q_{sr}	Capacity fade
SOC	State of charge in the electrode
SOH	State of health for the battery cell
T	Battery temperature
V	Terminal voltage
Parameters and subscripts:	
$-$	The negative electrode (Anode)
$+$	The positive electrode (Cathode)

With the nomenclature, given in Table D.1, the MPC formulation given in [7] and the reduced battery model described in Section 3.2.2, the following state vector

$$x := \begin{bmatrix} C_s^-, & q_s^-, & C_e^-, & T, & Q_{sr} \end{bmatrix}^T \tag{D.1}$$

is defined with input, u, representing the applied current. The output vector of interest is defined as

$$z := \begin{bmatrix} SOC, & SOH, & T, & V \end{bmatrix}^T. \tag{D.2}$$

The control-oriented battery model is summarized as

$$\dot{x}(t) = f^c(x(t), u(t)) \tag{D.3a}$$

$$z(t) = g(x(t), u(t)) := \begin{bmatrix} C_1 x(t) + c_1 \\ C_2 x(t) + c_2 \\ C_3 x(t) \\ h(x(t), u(t)) \end{bmatrix} \tag{D.3b}$$

where f^c, g, h are nonlinear functions, C_1, C_2, C_3 are constant matrices, and c_1, c_2 are constants.

To further reduce the computation complexity of the MPC charging controller, the nonlinear battery model in Equation (D.3) is linearized around the reference trajectory and previous system input, resulting in

$$x(i + 1) = A(i)x(i) + B(i)u(i) + d(i) \tag{D.4}$$

where

$$A(i) = \frac{\partial f(x(i), u(i-1))}{\partial x} \tag{D.5a}$$

$$B(i) = \frac{\partial f(x(i), u(i-1))}{\partial u} \tag{D.5b}$$

$$d(i) = f(x(i), u(i-1)) - A(i)x(i) - B(i)u(i-1). \tag{D.5c}$$

The linarized model is assumed to be invariant under the prediction horizon. Hence,

$$\begin{aligned} A(i) &\approx A_k, \quad B(i) \approx B_k \\ d(i) &\approx d_k, \quad \forall i \in \{0, ..., N-1\}. \end{aligned} \tag{D.6}$$

Input and state constraints:

The only input constraint in the system is

$$-I_{max} \leq u(i) \leq 0 \tag{D.7}$$

which limits the charging current up to some physically allowable limit. The following state constraints are considered in the charging problem:

$$C_{ss,min} \leq C_{ss}^{\pm}(i) \leq C_{ss,max} \tag{D.8a}$$

$$C_{e,min} \leq C_e^{\pm}(i) \leq C_{e,max} \tag{D.8b}$$

$$T(i) \leq T_{max} \tag{D.8c}$$

or in the compact form

$$Mx(i) \le c_0, \quad i \in \{1, ..., N - 1\}. \tag{D.9}$$

A vector of slack variables s is introduced to account for the uncertainty of the impact associated with explicit violations of these constraints. An additional term $s^T \Gamma s$ is added to the stage cost, and the state constraints are replaced by

$$Mx(i) \le c_0 + s \tag{D.10a}$$

$$s \ge 0 \tag{D.10b}$$

State estimation:

The estimator is based on the discretized battery model given in Equation (D.3):

$$\widehat{x}_{k+1} = f(\widehat{x}_k, u_k) + L_k \cdot [z_{k+1} - \widehat{z}_{k+1}] \tag{D.11a}$$

$$\widehat{z}_{k+1} = g(f(\widehat{x}_k, u_k), u_k) \tag{D.11b}$$

$$\widehat{y}_{k+1} = C\widehat{x}_{k+1} \tag{D.11c}$$

where the detail on the calculation of the estimator gain L_k can be found in [52].

References

[1] Siemens, "Snart blir trafikken over norske fjorder elektrisk," last Accessed: 4.12.2018. [Online]. Available: https://w3.siemens.no/home/no/no/topics/fremtiden-elektrisk/pages/elektrisk-bilferge.aspx

[2] Corvus Energy, "World's first all-electric car ferry," last Accessed: 5.12.2018. [Online]. Available: https://corvusenergy.com/marine-project/mf-ampere-ferry/

[3] Tersan Shipyard, "Nb1073 - battery powered ro-ro passenger & vehicle ferry / passengers vessels," 2016, last Accessed: 1.11.2018. [Online]. Available: http://www.tersanshipyard.com/projeler#NB1073

[4] K. W. Vadset, "Gloppefjord/eidsfjord," Maritimt Magasin, Mar. 2018, last Accessed: 1.11.2018. [Online]. Available: http://maritimt.com/nb/batomtaler/gloppefjordeidsfjord-032018

[5] Siemens, "Reference list - miscellaneous types of vessels," 2017, last Accessed: 1.11.2018. [Online]. Available: https://w3.siemens.no/home/no/no/sector/industry/marine/Documents/Miscellaneous-Types%20of-vessels-references_V2017.pdf

[6] "Været som var - sandane lufthamn målestasjon," Oct. 2018, last Accessed: 13.11.2018. [Online]. Available: https://www.yr.no/sted/Norge/Sogn_og_Fjordane/Gloppen/Sandane_lufthamn_m%C3%A5lestasjon/almanakk.html?dato=2018-09-26

[7] C. Zou, C. Manzie, and D. Nešić, "Model predictive control for lithium-ion battery optimal charging," *IEEE/ASME Transactions on Mechatronics*, vol. 23, no. 2, pp. 947–957, April 2018.

[8] M. Chediak, "The battery will kill fossil fuels—it's only a matter of time," Mar. 2018, last accessed: 12.09.2018. [Online]. Available: https://www.bloomberg.com/news/articles/2018-03-08/the-battery-will-kill-fossil-fuels-it-s-only-a-matter-of-time

[9] O. Moen, "Erfaringer så langt med drift og lading av «batteri-fartøy»," Apr. 2018, last Accessed: 12.12.2018. [Online]. Available: https://www.nek.no/wp-content/uploads/2018/05/9-14.00_Landstromsforum-Siemens-120418_Odd_Moen.pdf

[10] M. Holter and J. Hodges, "The next ferry you board might run on batteries," Mar. 2018, last accessed: 12.09.2018. [Online]. Available: https://www.bloomberg.com/news/features/2018-03-13/the-next-ship-you-board-might-run-on-batteries

[11] O. R. Valmot, "Slik fungerer batteriet som endret verden," Nov. 2013, last Accessed: 31.10.2018. [Online]. Available: https://www.tu.no/artikler/slik-fungerer-batteriet-som-endret-verden/233862

[12] W. Ying, Z. Zhi, A. Botterud, K. Zhang, and D. Qia, "Stochastic coordinated operation of wind and battery energy storage system considering battery degradation," *Journal of Modern Power Systems and Clean Energy*, vol. 4, no. 4, pp. 581–592, 2016.

[13] A. Barré, B. Deguilhem, S. Grolleau, M. Gérard, F. Suard, and D. Riu, "A review on lithium-ion battery ageing mechanisms and estimations for automotive applications," *Journal of Power Sources*, vol. 241, pp. 680 – 689, 2013. [Online]. Available: http://www.sciencedirect.com/science/article/pii/S0378775313008185

[14] F. Richter, P. J. Vie, S. Kjelstrup, and O. S. Burheim, "Measurements of ageing and thermal conductivity in a secondary nmc-hard carbon li-ion battery and the impact on internal temperature profiles," *Electrochimica Acta*, vol. 250, pp. 228 – 237, 2017. [Online]. Available: http://www.sciencedirect.com/science/article/pii/S0013468617316146

[15] Google Maps, "Lote-anda," Dec. 2018, last Accessed: 4.12.2018. [Online]. Available: https://www.google.com/maps/place/Lote-Anda/@61.854385,6.0790972,17z/data=!4m6!3m5!1s0x4616574ece03e449:0x5c026e1c198b2269!4b1!8m2!3d61.8543825!4d6.0812859

[16] Nordpool, "Day-ahead prices," Dec. 2018, last Accessed: 7.12.2018. [Online]. Available: https://www.nordpoolgroup.com/Market-data1/Dayahead/Area-Prices/ALL1/Hourly/?view=table

[17] Finanskomiteen, "Innst. 2 s tillegg 1," Nov. 2014, last accessed: 10.09.2018. [Online]. Available: https://www.stortinget.no/globalassets/pdf/innstillinger/stortinget/2014-2015/inns-201415-002-t001.pdf

[18] DNV GL, "Elektrifisering av bilferger i norge – kartlegging av investeringsbehov i strømnettet," May 2015, last accessed: 12.09.2018. [Online]. Available: https://www.energinorge.no/contentassets/0ae3a2b651ae4e83a0487ad493c3270c/elektrifisering-av-bilferger-i-norge.pdf

[19] Norwegian Ministry of Climate and Environment, "Law on climate goals (climate act)," Jun. 2017, last accessed: 12.09.2018. [Online]. Available: https://lovdata.no/dokument/NL/lov/2017-06-16-60

[20] T. Randall and J. Lippert, "Tesla's newest promises break the laws of batteries," Nov. 2017, last accessed: 14.09.2018. [Online]. Available: https://www.bloomberg.com/news/articles/2017-11-24/tesla-s-newest-promises-break-the-laws-of-batteries

[21] T. Stensvold, "Siemens: Lønnsomt å bytte ut 70 prosent av fergene med batteri- eller hybridferger," Aug. 2015, last accessed: 14.09.2018. [Online]. Available: https://www.tu.no/artikler/siemens-lonnsomt-a-bytte-ut-70-prosent-av-fergene-med-batteri-eller-hybridferger/196845

[22] J. Madslien, "Pining for cleaner air in the norwegian fjords," Apr. 2017, last accessed: 26.09.2018. [Online]. Available: https://www.bbc.com/news/business-39478856

[23] E. Skjong, R. Volden, E. Rødskar, M. Molinas, T. A. Johansen, and J. Cunningham, "Past, present, and future challenges of the marine vessel's electrical power system," *IEEE Transactions on Transportation Electrification*, vol. 2, no. 4, pp. 522–537, Dec 2016.

[24] E. Skjong, T. A. Johansen, M. Molinas, and A. J. Sørensen, "Approaches to economic energy management in diesel–electric marine vessels," *IEEE Transactions on Transportation Electrification*, vol. 3, no. 1, pp. 22–35, March 2017.

[25] M. Broussely, S. Herreyre, P. Biensan, P. Kasztejna, K. Nechev, and R. Staniewicz, "Aging mechanism in li ion cells and calendar life predictions," *Journal of Power Sources*, vol. 97-98, pp. 13 – 21, 2001, proceedings of the 10th International Meeting on Lithium Batteries. [Online]. Available: http://www.sciencedirect.com/science/article/pii/S0378775301007224

[26] I. Bloom, B. Cole, J. Sohn, S. Jones, E. Polzin, V. Battaglia, G. Henriksen, C. Motloch, R. Richardson, T. Unkelhaeuser, D. Ingersoll, and H. Case, "An accelerated calendar and cycle life study of li-ion cells," *Journal of Power Sources*, vol. 101, no. 2, pp. 238 – 247, 2001. [Online]. Available: http://www.sciencedirect.com/science/article/pii/S0378775301007832

[27] R. Suresh and R. Rengaswamy, "Modeling and control of battery systems. part ii: A model predictive controller for optimal charging," *Computers & Chemical Engineering*, vol. 119, pp. 326–335, 2018.

[28] A. Abdollahi, X. Han, G. Avvari, N. Raghunathan, B. Balasingam, K. Pattipati, and Y. Bar-Shalom, "Optimal battery charging, part i: Minimizing time-to-charge, energy loss, and temperature rise for ocv-resistance battery model," *Journal of Power Sources*, vol. 303, pp. 388 – 398, 2016. [Online]. Available: http://www.sciencedirect.com/science/article/pii/S0378775315003092

[29] A. Abdollahi, X. Han, N. Raghunathan, B. Pattipati, B. Balasingam, K. Pattipati, Y. Bar-Shalom, and B. Card, "Optimal charging for general equivalent electrical battery model, and battery life management," *Journal of Energy Storage*, vol. 9, pp. 47 – 58, 2017. [Online]. Available: http://www.sciencedirect.com/science/article/pii/S2352152X16302419

[30] Ships of CalMac, "Hallaig: History," Nov. 2013, last Accessed: 17.12.2018. [Online]. Available: http://www.shipsofcalmac.co.uk/h_hallaig.asp

[31] J. A. Suul, "Introduction to marine power systems and control of power electronic converters," Aug. 2018.

[32] M. Patel, *Shipboard electrical power systems*.   CRC Press, 2012.

[33] . Grøn, "skinneffekt," Feb. 2009, last Accessed: 4.12.2018. [Online]. Available: https://snl.no/skinneffekt

[34] V. Staudt, R. Bartelt, and C. Heising, "Fault scenarios in dc ship grids: The advantages and disadvantages of modular multilevel converters." *IEEE Electrification Magazine*, vol. 3, no. 2, pp. 40–48, June 2015.

[35] R. Geertsma, R. Negenborn, K. Visser, and J. Hopman, "Design and control of hybrid power and propulsion systems for smart ships: A review of developments," *Applied Energy*, vol. 194, pp. 30–54, 2017.

[36] R. Prenc, A. Cuculić, and I. Baumgartner, "Advantages of using a dc power system on board ship," *Pomorski zbornik*, vol. 52, no. 1, pp. 83–97, 2016. [Online]. Available: https://hrcak.srce.hr/index.php?id_clanak_jezik=251458&show=clanak

[37] B. Lawson, "Primary (non rechargeable) batteries," 2005, last accessed: 31.10.2018. [Online]. Available: https://www.mpoweruk.com/primary.htm

[38] ——, "Secondary (rechargeable) batteries," 2005, last accessed: 31.10.2018. [Online]. Available: https://www.mpoweruk.com/secondary.htm

[39] ——, "Battery performance characteristics," 2005, last Accessed: 5.12.2018. [Online]. Available: https://www.mpoweruk.com/performance.htm

[40] ——, "Lead acid batteries," 2005, last accessed: 31.10.2018. [Online]. Available: https://www.mpoweruk.com/lithiumS.htm

[41] ——, "Nickel metal hydride batteries," 2005, last accessed: 31.10.2018. [Online]. Available: https://www.mpoweruk.com/nimh.htm

[42] ——, "Rechargeable lithium batteries," 2005, last accessed: 31.10.2018. [Online]. Available: https://www.mpoweruk.com/leadacid.htm

[43] S. Bashash, S. J. Moura, J. C. Forman, and H. K. Fathy, "Plug-in hybrid electric vehicle charge pattern optimization for energy cost and battery longevity," *Journal of Power Sources*, vol. 196, no. 1, pp. 541 – 549, 2011. [Online]. Available: http://www.sciencedirect.com/science/article/pii/S0378775310011390

[44] I. Buchmann, "Bu-205: Types of lithium-ion," 2018, last Accessed: 31.10.2018. [Online]. Available: https://batteryuniversity.com/learn/article/types_of_lithium_ion

[45] J. Jiang and C. Zhang, *Fundamentals and applications of lithium-ion batteries in electric drive vehicles*, S. P. Services, Ed.   Singapore: John Wiley & Sons Inc., 2015.

[46] Y. Cui, C. Du, G. Yin, Y. Gao, L. Zhang, T. Guan, L. Yang, and F. Wang, "Multi-stress factor model for cycle lifetime prediction of lithium ion batteries with shallow-depth discharge," *Journal of Power Sources*, vol. 279, pp. 123–132, 2015.

[47] Norled AS, "E39 lavik - oppedal," Nov. 2018, last Accessed: 13.11.2018. [Online]. Available: https://www.norled.no/contentassets/ a4aa7bd2b2304c6d8aaf5df4c97a4d94/lavik-oppedal_rute1046_k3-2018.pdf

[48] The MathWorks, Inc., "Simulink," Dec. 2018, last Accessed: 8.12.2018. [Online]. Available: https://se.mathworks.com/products/simulink.html

[49] D. Mayne, J. Rawlings, C. Rao, and P. Scokaert, "Constrained model predictive control: Stability and optimality," *Automatica*, vol. 36, no. 6, pp. 789 – 814, 2000. [Online]. Available: http://www.sciencedirect.com/science/article/pii/ S0005109899002149

[50] B. Foss and T. A. N. Heirung, "Merging optimization and control," *Lecture Notes*, 2013.

[51] R. C. Cope and Y. Podrazhansky, "The art of battery charging," in *Fourteenth Annual Battery Conference on Applications and Advances. Proceedings of the Conference (Cat. No.99TH8371)*, Jan 1999, pp. 233–235.

[52] C. Zou, C. Manzie, D. Nešić, and A. G. Kallapur, "Multi-time-scale observer design for state-of-charge and state-of-health of a lithium-ion battery," *Journal of Power Sources*, vol. 335, pp. 121 – 130, 2016. [Online]. Available: http://www.sciencedirect.com/science/article/pii/S037877531631432X

[53] Y. He, B. Venkatesh, and L. Guan, "Optimal scheduling for charging and discharging of electric vehicles," *IEEE Transactions on Smart Grid*, vol. 3, no. 3, pp. 1095–1105, Sept 2012.